# Quantum correlations on the no-signaling boundary: self-testing and more

Kai-Siang Chen,<sup>1</sup> Gelo Noel M. Tabia,<sup>1,2,3</sup> Chellasamy Jebarathinam,<sup>4</sup> Shiladitya Mal,<sup>1,2</sup> Jun-Yi Wu,<sup>5</sup> and Yeong-Cherng Liang<sup>1,2,\*</sup>

<sup>1</sup>Department of Physics and Center for Quantum Frontiers of Research & Technology (QFort), National Cheng Kung University, Tainan 701, Taiwan

<sup>2</sup>Physics Division, National Center for Theoretical Sciences, Taipei 10617, Taiwan

<sup>3</sup>Center for Quantum Technology, National Tsing Hua University, Hsinchu 300, Taiwan

<sup>4</sup>Center for Theoretical Physics, Polish Academy of Sciences, Aleja Lotników 32/46, 02-668 Warsaw, Poland

<sup>5</sup>Department of Physics, Tamkang University, Tamsui, New Taipei 251301, Taiwan

(Dated: September 16, 2022)

In device-independent quantum information, correlations between local measurement outcomes observed by spatially separated parties in a Bell test play a fundamental role. Even though it is long-known that the set of correlations allowed in quantum theory lies strictly between the Bell-local set and the no-signaling set, many questions concerning the geometry of the quantum set remain unanswered. Here, we revisit the problem of when the boundary of the quantum set coincides with the no-signaling set in the simplest Bell scenario. In particular, we prove that self-testing is possible in nontrivial classes of these common boundaries beyond the known examples of Hardy-type correlations and provide numerical evidence supporting the robustness of these self-testing results. As a byproduct, we also show that if the qubit strategies leading to an extremal nonlocal correlation are local-unitarily equivalent, a self-testing statement based on this correlation follows. Interestingly, all these self-testing correlations found on the no-signaling boundary are provably non-exposed. An analogous characterization for the set  $\mathcal M$  of quantum correlations arising from finite-dimensional maximally entangled states is also provided. En route to establishing this last result, we show that all correlations of  $\mathcal M$  in the simplest Bell scenario are attainable as convex combinations of those achievable using a Bell pair and projective measurements. In turn, we obtain the maximal Clauser-Horne-Shimony-Holt Bell inequality violation by any maximally entangled two-qudit state and a no-go theorem regarding the self-testing of such states.

### I. INTRODUCTION

In the context of a Bell test, the principle of relativistic causality [1], as proposed by Popescu and Rohrlich, demands that it is impossible to perform superluminal communication between spatially separated parties via their choice of measurements. Interestingly, it was shown in [1] that this principle alone (or even in conjunction with some other principles [2–5]) is insufficient in demarcating precisely the boundary of the quantum set  $\mathcal Q$  of correlations. In contrast, although Bell's principle of local causality [6] is also very wellmotivated, it is too restrictive since quantum correlations arising from certain entangled quantum states are known [7] to be incompatible with the constraints (known by the name of Bell inequalities) derived therefrom.

By now, it is well-known that Bell-nonlocality (hereafter abbreviated as nonlocality), i.e., the possibility of exhibiting correlations stronger than that allowed by local causality, is an indispensable resource for device-independent (DI) quantum information (QI) [8, 9]. In other words, the fact that some entangled states can generate nonlocal correlation guarantees its usefulness in some DI quantum information processing protocols, such as quantum key distribution [10] and random number generation [11, 12]. More generally, even though we make no assumptions about the internal workings of the devices in a DI analysis, we can infer nontrivial conclusions about the employed devices directly from the observed correlations,

see, e.g., [13–24]. In some cases, one can even perform self-testing [25] of the devices, confirming that the devices work as expected, modulo unimportant local degrees of freedom. See [26] for a recent review and, in particular, [27–32] for some recent experimental demonstrations and challenges.

In the bipartite scenario, the principle of relativistic causality gives rise to the no-signaling (NS) conditions [33] (see, however, [34]), and hence the set of  $\mathcal{NS}$  correlations. Since  $\mathcal{Q}$  is a strict subset of  $\mathcal{NS}$ , the quantum advantage offered by any entangled state is constrained by the NS conditions. In particular, it would be interesting to understand when the power of a quantum resource is constrained exactly *only* by these conditions. Geometrically [35], this amounts to determining when the boundary of  $\mathcal{Q}$  meets that of  $\mathcal{NS}$ , beyond trivial instances when they also meet the boundary of the Bell-local set.

A well-known nonlocal example of a correlation lying on these common boundaries is that introduced in the context of the Hardy paradox [36], which demonstrates nonlocality without resorting to any Bell inequality. Intriguingly, Hardy's argument applies to all *but* the maximally entangled two-qubit state. In fact, as we see in this work, even a maximally entangled state of an arbitrary finite Hilbert space dimension cannot exhibit the original Hardy paradox (see, however, Proposition 9 of [37], where the authors proposed Hardy-type paradox for all *except* the two-qubit maximally entangled states).

The above observation manifests the difference between  $\mathcal{Q}$  and  $\mathcal{M}$  (the convex hull of the set of correlations attainable by finite-dimensional maximally entangled states). In this work, we revisit the problem of characterizing—in the simplest Bell scenario—when the boundary of  $\mathcal{Q}$ , as well as  $\mathcal{M}$  meet the boundary of  $\mathcal{NS}$ . The former characterization can be deduced

<sup>\*</sup> ycliang@mail.ncku.edu.tw

also from the findings of [38], but we provide in addition explicit strategies for their quantum realization.

Another interesting feature of Hardy's correlation is that it can be used to self-test [39], and hence certify that the underlying quantum strategy is essentially unique. Since then, other examples of correlations [40, 41] showing a Hardy-type paradox were also shown [42, 43] to be a self-test. Here, we show that for all the other nontrivial Classes of common boundaries between  $\mathcal{Q}$  and  $\mathcal{NS}$ , one can similarly find self-testing correlations. Moreover, all these examples, as with the Hardy correlation [35], are provably non-exposed points.

We structure the rest of this paper as follows. In Section II, we introduce formally the various sets of correlations alluded to above and the other basic knowledge required for our analysis. Then, in Section III, we provide an alternative characterization of the common boundary of  $\mathcal Q$  and  $\mathcal N\mathcal S$ , as well as examples of nonlocal quantum correlations lying on them that can be self-tested. In Section IV, we prove a Lemma concerning the extreme points of the set of correlations due to finite-dimensional maximally entangled state in the simplest Bell scenario. We then use this to prove, for such states, the maximal Clauser-Horne-Shimony-Holt [44] Bell inequality violation and a no-go theorem for their self-testing. In Section V, we summarize the results obtained and outline some possible directions for future research.

## II. PRELIMINARIES

#### A. Sets of correlations

In the simplest Bell scenario, two experimenters (Alice and Bob) may perform two dichotomic measurements each. The correlation between the local measurement outcomes may be summarized [8] by a collection of joint conditional probability distributions  $\vec{P} = \{P(a,b|x,y)\}_{x,y,a,b=0,1}$  where a and b (x and y) are, respectively, the label for the measurement outcome (setting) for the first and the second party.

Note that entries of  $\vec{P}$  have to satisfy certain mathematical as well as physical constraints. For example, a probability distribution has to be non-negative and normalized, so

$$P(a, b|x, y) \ge 0 \quad \forall \ a, b, x, y, \tag{1a}$$

$$\sum_{a,b} P(a,b|x,y) = 1, \quad \forall \ x,y. \tag{1b}$$

In addition, we are exclusively interested only in the set  $\mathcal{NS}$ , i.e., the set of correlations that satisfy the NS conditions [33]

$$\sum_{a} P(a, b|x, y) = \sum_{a} P(a, b|x', y) \ \forall \ x, x', b, y$$

$$\sum_{b} P(a, b|x, y) = \sum_{b} P(a, b|x, y') \ \forall \ y, y', a, x.$$
(2)

These set of all such correlations forms a convex polytope. In particular, within the subspace of  $\vec{P}$  satisfying Eq. (2),  $\mathcal{NS}$  is fully characterized by "positivity facets", i.e., those inequalities given in Eq. (1a). In the simplest Bell scenario,  $\mathcal{NS}$  is spanned by 24 vertices, 16 of which are Bell-local (or simply *local*), while the remaining 8 take the form of [33]:

$$P(a,b|x,y) = \frac{1}{2}\delta_{a\oplus b,xy\oplus\alpha x\oplus\beta y\oplus\gamma}$$
 (3)

where  $\delta_{c,d}$  is the Kronecker delta between c and d, and  $\alpha, \beta, \gamma \in \{0, 1\}$  are free parameters characterizing these non-local extremal points. In honor of the pioneering work of Popescu and Rohrlich (PR) [1], these nonlocal extremal points are referred to as PR boxes [33].

In contrast, the convex hull of the 16 local extremal points gives the so-called Bell polytope, or the local polytope, which we denote by  $\mathcal{L}$ . This is the set of correlations allowed by a local hidden variable theory [7], or equivalently the set of correlations that respects the principle of local causality [6]

$$P(a, b|x, y) = \sum_{\lambda} q_{\lambda} p(a|x, \lambda) p(b|y, \lambda) \quad \forall x, y, \quad (4)$$

where the local response functions  $p(a|x, \lambda), p(b|y, \lambda)$  can be taken, without loss of generality, to be either 0 or 1, and  $\lambda$  can be understood as the local hidden variable (or computationally as a label for the extreme points of the local polytope).

In this simplest Bell scenario, the Bell polytope is equivalently characterized by 16 positivity facets and 8 facet-defining Bell inequalities [45], first discovered by Clauser-Horne-Shimony-Holt (CHSH) [44]. Consequently, this Bell scenario is often referred to as the CHSH Bell scenario. For subsequent discussions, the following CHSH (Bell) inequality is of particular relevance:

$$S_{\text{CHSH}} = \sum_{x,y,a,b=0}^{1} (-1)^{xy+a+b+1} P(a,b|x,y) \stackrel{\mathcal{L}}{\leq} 2 \quad (5)$$

The very basis of DIQI is that not all quantum correlations, namely, those obtained by performing local measurements on a shared quantum state  $\rho$  can be decomposed in the form of Eq. (4). Formally, the set of quantum correlations  $\mathcal Q$  consists of all  $\vec P$  that respect Born's rule:

$$P(a,b|x,y) = \operatorname{tr}[(M_{a|x}^A \otimes M_{b|y}^B)\rho], \tag{6}$$

where  $M_{a|x}^A$  and  $M_{b|y}^B$  are, respectively, the positive operator-valued measure (POVM) elements associated with Alice's and Bob's local measurements. Notice that there is no restriction on the local Hilbert space dimension in Eq. (6). Thus, by Neumark's theorem [46], we can always take the POVM elements to be projectors when deciding whether a given  $\vec{P}$  is in  $\mathcal{Q}$ .

<sup>&</sup>lt;sup>1</sup> A facet of a polytope  $\mathcal{P}$  is a boundary of  $\mathcal{P}$  having maximal dimension.

Within Q, a set of particular interest is the set of correlations attainable by finite-dimensional maximally entangled states, i.e.,  $\rho = |\Phi_d^+\rangle\langle\Phi_d^+|$  with

$$|\Phi_d^+\rangle = \frac{1}{\sqrt{d}} \sum_{i=0}^{d-1} |i\rangle|i\rangle, \quad 2 \le d < \infty.$$
 (7)

For each  $d \geq 2$ , we denote by  $\mathcal{M}_d$  the convex hull of the set of all correlations attainable by  $|\Phi_d^+\rangle$  via Eq. (6) and by  $\mathcal{M}$  the convex hull of the union  $\cup_{d=2,3,...}\mathcal{M}_d$ . From Eq. (6), it follows that for any such states

$$P(a, b|x, y) = \frac{1}{d} \operatorname{tr} \left[ M_{a|x}^A \left( M_{b|y}^B \right)^{\mathsf{T}} \right] = \frac{1}{d} \operatorname{tr} \left[ \left( M_{a|x}^A \right)^{\mathsf{T}} M_{b|y}^B \right],$$
(8)

where  $^{\text{T}}$  denotes the transposition operation. Clearly,  $\mathcal{M} \subsetneq \mathcal{Q}$ , and the fact that the inclusion is generally strict was shown independently in [47], [48], and [49] (see also [50] and [51]).

In the CHSH Bell scenario, it is expedient to consider also the correlator, which is the probability of getting the same outcome minus the probability of getting different outcomes:

$$\langle A_x B_y \rangle := \sum_{a,b=0}^{1} (-1)^{a+b} P(a,b|x,y).$$
 (9)

In quantum theory, this corresponds to the expectation value  $\langle A_x B_y \rangle = \operatorname{tr}(A_x \otimes B_y \rho)$  where

$$A_x := M_{0|x}^A - M_{1|x}^A, \quad B_y := M_{0|y}^B - M_{1|y}^B \tag{10}$$

are both dichotomic observables (i.e., with  $\pm 1$  eigenvalues). From Eq. (10), we can also express the POVM elements for all  $x, y, a, b \in \{0, 1\}$  in terms of the observables as

$$M_{a|x}^A = \frac{\mathbb{1}_2 + (-1)^a A_x}{2}$$
 and  $M_{b|y}^B = \frac{\mathbb{1}_2 + (-1)^b B_y}{2}$ . (11)

# B. Self-testing

One of our interests is to show that nonlocal correlations lying on the common boundaries of  $\mathcal Q$  and  $\mathcal N\mathcal S$  can be used to self-test [26] certain reference state and measurements. For completeness, we now recall from [35] the following definition for self-testing of states and measurements.

**Definition II.1** (Self-testing). A quantum correlation  $\vec{P} \in \mathcal{Q}$  is said to self-test the reference quantum realization  $\{|\widetilde{\psi}\rangle, \{\widetilde{M_{a|x}^A}\}, \{\widetilde{M_{b|y}^B}\}\}$  of  $\vec{P}$  if for all states  $|\psi\rangle_{AB}$  and measurements  $\{M_{a|x}^A\}, \{M_{b|y}^B\}$  giving the same correlation  $\vec{P}$ , one can find  $\Phi := \Phi_A \otimes \Phi_B$  with local isometries  $\Phi_A : \mathcal{H}_A \mapsto \mathcal{H}_{A'} \otimes \mathcal{H}_{A''}$  and  $\Phi_B : \mathcal{H}_B \mapsto \mathcal{H}_{B'} \otimes \mathcal{H}_{B''}$  such that

$$\Phi(M_{a|x}^{A} \otimes M_{b|y}^{B} | \psi \rangle_{AB}) = |\varsigma\rangle_{A'B'} \otimes \widetilde{M_{a|x}^{A}} \otimes \widetilde{M_{b|y}^{B}} | \widetilde{\psi}\rangle_{A''B''}, \tag{12a}$$

holds for some auxiliary "junk" state  $|\varsigma\rangle_{A'B'}$ . By summing over all a, b and using the linearity of  $\Phi$ , one also obtains the usual self-testing requirement for a state

$$\Phi(|\psi\rangle_{AB}) = |\varsigma\rangle_{A'B'} \otimes |\widetilde{\psi}\rangle_{A''B''} \,. \tag{12b}$$

Notice that there are examples of  $\vec{P} \in \mathcal{Q}$  that self-test a reference state but not the underlying measurements, see, e.g., [52–54]. Furthermore, in the CHSH Bell scenario, a self-testing quantum correlation is necessarily extremal [35] in  $\mathcal{Q}$ .

Let us now recall from [55] the following characterization of the extreme points of Q applicable to this Bell scenario.

**Fact II.2** (Masanes [55]). In an N-partite Bell scenario involving only two dichotomic measurements, all extreme points of Q are achievable by measuring N-qubit pure states with projective measurements.

With Fact II.2 in mind, it seems natural to first understand whether seemingly different qubit strategies for realizing a given correlation  $\vec{P}$  are indeed different. To this end, we introduce the following definition to capture equivalence classes of quantum strategies.

**Definition II.3** (d-equivalent). A quantum realization of  $\vec{P}$  consisting of  $\left\{ |\psi\rangle, \{M_{a|x}^A\}, \{M_{b|y}^B\} \right\}$  is said to be dequivalent to another quantum realization of  $\vec{P}$  given by  $\left\{ |\tilde{\psi}\rangle, \{\widetilde{M_{a|x}^A}\}, \{\widetilde{M_{b|y}^B}\} \right\}$  if there exist d-dimensional local unitary operators  $u_A$  and  $u_B$  such that

$$u_A \otimes u_B |\psi\rangle = |\tilde{\psi}\rangle,$$
 (13a)

$$u_A \otimes u_B(M_{a|x}^A \otimes M_{b|y}^B) u_A^{\dagger} \otimes u_B^{\dagger} = \widetilde{M_{a|x}^A} \otimes \widetilde{M_{b|y}^B}. \quad (13b)$$

From Eq. (6), d-equivalent quantum strategies clearly result in the same correlation  $\vec{P}$ . The converse, however, is not necessarily true. To show that a given  $\vec{P}$  in the CHSH Bell scenario is a self-test, it thus seems natural—given Fact II.2—to first determine if all qubit strategies realizing  $\vec{P}$  are 2-equivalent. If so, the following Theorem allows one to promote such an observation to a self-testing statement.

**Theorem II.4.** In the CHSH Bell scenario, if all qubit strategies  $\left\{|\psi\rangle\,,\{M_{a|x}^A\},\{M_{b|y}^B\}\right\}$  giving an extremal nonlocal correlation  $\vec{P}$  are 2-equivalent to a specific reference strategy  $\left\{|\tilde{\psi}\rangle\,,\{\widetilde{M_{a|x}^A}\},\{\widetilde{M_{b|y}^B}\}\right\}$ , then  $\vec{P}$  self-tests the quantum realization given by this reference strategy.

For a proof of the Theorem, see Appendix A.

## C. Correlation tables and relabeling

A correlation  $\vec{P}$  is conveniently represented using a table showing all entries of  $\vec{P}$ , as shown in Table I. Note that the non-negativity requirement of Eq. (1a) demands that all entries in the correlation table are non-negative. The normalization requirement of Eq. (1b), on the other hand, means that within each block corresponding to a fixed value of x, y, the sum of all entries gives one.

For the rest of the paper, it is worth remembering that a relabeling of the measurement settings x (y), the measurement outcomes a (b), or the parties Alice  $\leftrightarrow$  Bob does not lead to

	x = 0	x = 1
	a = 0   a = 1	a = 0   a = 1
$y = 0 \begin{vmatrix} b = 0 \\ b = 1 \end{vmatrix}$	δ	
$y = 1 \begin{vmatrix} b = 0 \\ b = 1 \end{vmatrix}$		

Table I: A correlation table showing the entries of a correlation  $\vec{P}$ . For instance, if the probability of getting outcomes a=1,b=0 for the given settings x=0,y=0 is  $\delta$ , we write  $P(1,0|0,0)=\delta$ , or equivalently, a  $\delta$  as the corresponding entry in the correlation table. To simplify presentation, we omit "a=", "b=", and the lines separating the different outcomes in all the correlation tables presented below.

any change in the nature of the correlation. In other words, if  $\vec{P}$  is a member of  $\mathcal{L}$ ,  $\mathcal{Q}$ , or  $\mathcal{NS}$ , it remains so after any such relabeling or even combinations thereof. In the context of the correlation table, cf. Table I, a relabeling of the measurement settings  $x=0 \leftrightarrow x=1$  amounts to interchanging the two block columns (consisting of two columns each) whereas a relabeling of the measurement outcomes  $a=0 \leftrightarrow a=1$  for some given value of x amounts to swapping the two columns associated with that value of x. Similarly, a relabeling of Bob's measurement settings  $y=0 \leftrightarrow y=1$  or his outcome  $b=0 \leftrightarrow b=1$  entails a permutation of the corresponding rows in the table. Finally, a relabeling of the parties amounts to performing a transposition of the table.

# D. A signature of Bell-local correlations

When seen as a convex combination of the extreme points of  $\mathcal{NS}$ , any correlation  $\vec{P}$  lying outside the local polytope, i.e.,  $\vec{P} \notin \mathcal{L}$  must have contribution(s) from at least one PR box, such as that shown in Eq. (14).

$$\vec{P}_{PR} := \begin{array}{c|cccc} & x = 0 & x = 1 \\ \hline 0 & 1 & 0 & 1 \\ \hline y = 0 & 0 & 0 & \frac{1}{2} & 0 & \frac{1}{2} \\ \hline 1 & \frac{1}{2} & 0 & \frac{1}{2} & 0 \\ \hline y = 1 & 0 & 0 & \frac{1}{2} & \frac{1}{2} & 0 \\ 1 & \frac{1}{2} & 0 & 0 & \frac{1}{2} \end{array}$$
 (14)

A distinctive feature of the PR box correlation shown in Eq. (14) is that it consists of three anti-diagonal blocks satisyfing xy=0 and one diagonal block for x=y=1. Or equivalently,  $\vec{P}_{PR}$  consists of three blocks of diagonal zeros (DZs) and one of block anti-diagonal zeros (ADZs). Moreover, all non-vanishing entries are  $\frac{1}{2}$ . With some thought, it is easy to see that all the other PR boxes, which can be obtained via a relabeling from Eq. (14), must have either (i) three blocks of DZs and one block of ADZs [like the one shown in Eq. (14)] or (ii) three blocks of ADZs and one block of DZs.

Since any nontrivial convex combination of non-negative numbers is non-vanishing, the above observations imply that a  $\vec{P}$  containing two neighboring zeros within a block (such as that shown in Table IIc and Table IId) cannot have a nontrivial contribution from a PR box. Hence, as was already noted in [56], we have the following simple sufficient condition for a given  $\vec{P}$  to be in  $\mathcal{L}$ .

**Observation II.5.** In the simplest Bell scenario, if the correlation table for a certain  $\vec{P} \in \mathcal{NS}$  has two neighboring zeros within a block, then  $\vec{P}$  is necessarily Bell-local, i.e.,  $\vec{P} \in \mathcal{L}$ .

For example, the local deterministic correlation  $P(a,b|x,y) = \delta_{a,x}\delta_{b,y}$ , which is an extreme point of both  $\mathcal L$  and  $\mathcal N\mathcal S$ , has neighboring zeros in every block. Observation II.5, of course, allows one to identify  $\vec P \in \mathcal L$  beyond such trivial examples.

Finally, note that each (positivity) facet of  $\mathcal{NS}$  is characterized by having exactly one joint conditional probability distribution P(a,b|x,y) being identically zero, i.e., when exactly one out of the 16 inequalities of Eq. (1a) is saturated. Consequently, when n of the entries of  $\vec{P}$  vanish, the correlation  $\vec{P}$  lies at the intersection of n such positivity facets of  $\mathcal{NS}$ . In other words, a given  $\vec{P} \in \mathcal{Q}$  belongs to the boundary of  $\mathcal{NS}$  if at least one of its entries in  $\{P(a,b|x,y)\}_{x,y,a,b=0,1}$  is zero.

# III. WHEN THE BOUNDARY OF $\mathcal Q$ MEETS THE BOUNDARY OF $\mathcal N\mathcal S$

In this section, we proceed to classify the different possibilities of when a correlation  $\vec{P}$  lying on the quantum boundary also sits on the no-signaling boundary. Our classification, inspired by the work of Fritz [56], is based on the different number of zeros appearing in the correlation table. Specifically, we prove, independently of [38], whether such correlations are necessarily local and provide an explicit example of a quantum strategy realizing a member from each class.

Since  $\mathcal{Q}$  is the convex hull of its extreme points, it follows from Fact II.2 that *if no* two-qubit pure state with projective measurements can generate a correlation table having zeros at the designated positions, then the corresponding correlation  $\vec{P}$  must lie outside  $\mathcal{Q}$ . Similarly, *if all* two-qubit states with projective measurements giving rise to k zeros ( $k \in \{1, 2, ...\}$ ) at some designated positions in a correlation table are such that the corresponding  $\vec{P} \in \mathcal{L}$ , then there is *no* quantum  $\vec{P}$  outside  $\mathcal{L}$  giving the same set of zeros in the correlation table. Therefore, for the present purpose, it suffices to restrict to qubit strategy in conjunction with projective measurements, even though the set of dimension-restricted quantum correlations is known generally to be concave (see, e.g., Refs. [35, 57, 58]).

## A. Further signature of local quantum correlations

With the above observations, we arrive at our first result.

**Lemma III.1.** In the CHSH Bell scenario, if there are two (or more) zeros in the same row (or column) of the correlation table, then the corresponding quantum correlation is local.

	<i>x</i> =	= 0	x =	= 1
	0	1	0	1
y = 0	0			
y = 0		0		
y=1 0				
y-1				

(a) Zeros at t	e diagonal	posi-
tions (DZs).		

	x = 0		x =	= 1
	0	1	0	1
y = 0		0		
y = 0	0			
y=1				
y-1				

(b) Zeros at the anti-diagonal positions (ADZs).

	<i>x</i> =	= 0	<i>x</i> =	= 1
	0	1	0	1
$y = 0 \begin{array}{c} 0 \\ 1 \end{array}$	0	0		
y=1 $0$ $1$				

(c	) Zeros	on	the	same	row.

	x = 0	$0 \mid x = 1 \mid$
	0 1	0 1
y=0	0	
y = 0	0	
y=1		
y=1		

(d) Zeros on the same column.

Table II: All possibilities of correlation tables with two zeros in the same block (shown here for x = y = 0).

*Proof.* Given Observation II.5, it remains to consider correlation tables having two zeros in the same row (or column) but different blocks. By relabeling, they take the form of Table III.

	x =	= 0	<i>x</i> =	= 1
	0	1	0	1
y=0	0		0	
y = 0				
y=1 0				
y-1				

Table III: A correlation table with two zeros in the same row but different blocks.

Then, it suffices to show that all extreme points of Q having the same two zeros as in Table III are local.

For the realization of these extreme points, we may consider, by Fact II.2, a 2-qubit pure state in conjunction with projective measurements. Note, however, that if any of these POVM elements is full rank, the resulting quantum correlation is necessarily local (see, e.g., Appendix B.3.1 of [59]). Hence, we consider hereafter only rank-one projective measurements in the orthonormal bases

$$\{|e_{0|x}\rangle, |e_{1|x}\rangle\}_{x=0,1} \text{ for Alice},$$
and 
$$\{|f_{0|y}\rangle, |f_{1|y}\rangle\}_{y=0,1} \text{ for Bob},$$
(15)

or equivalently, dichotomic observables [Eq. (10)]:

$$A_{x} = |e_{0|x}\rangle\langle e_{0|x}| - |e_{1|x}\rangle\langle e_{1|x}|, B_{y} = |f_{0|y}\rangle\langle f_{0|y}| - |f_{1|y}\rangle\langle f_{1|y}|.$$
 (16)

By the completeness of these bases, we may express a generic bipartite two-qubit pure state as :

$$|\Psi\rangle = \sum_{a,b=0}^{1} c_{ab} |e_{a|0}\rangle |f_{b|0}\rangle \tag{17}$$

where  $c_{ab} \in \mathbb{C}$ . To satisfy P(0,0|0,0) = 0, we must have  $c_{00} = 0$ , then

$$|\Psi\rangle = c_{10} |e_{1|0}\rangle |f_{0|0}\rangle + c_{01} |e_{0|0}\rangle |f_{1|0}\rangle + c_{11} |e_{1|0}\rangle |f_{1|0}\rangle.$$
(18)

Now, either  $c_{10}=0$  or  $1\geq |c_{10}|>0$ . For the former, the quantum state is separable state and the resulting correlation  $\vec{P}$  must be [60] local. For the latter, the requirement of P(0,0|1,0)=0 together with Eq. (6), Eq. (15), and Eq. (18) imply that  $\langle e_{0|1}|e_{1|0}\rangle=0$ . This means that Alice's two measurements are identical up to a relabeling of the outcome, i.e., they are jointly measurable [61]. Hence, there exists a joint distribution involving both settings of Alice. By the celebrated result of Fine [62], the resulting correlation is again local. Since all extreme points of  $\mathcal Q$  having the same two zeros are local, so must their convex mixtures, which completes the proof of the Lemma.

Lemma III.1 implies that a nonlocal quantum correlation *cannot* have more than one zero in any row or column, or more than four zeros in total in its correlation table. Note, however, that correlation tables having more zeros may not even be realizable quantum mechanically. For example, a correlation table having more than twelve zeros is nonphysical whereas that having exactly eleven zeros must violate the NS conditions of Eq. (2).

Hereafter, we focus on characterizing the boundary of  $\mathcal Q$  where the corresponding correlation table contains four or less zeros. In particular, we are interested to know when each of these cases contain also nonlocal quantum correlations and whether they lead to self-testing statements. Again, given Lemma III.1, we do not consider classes having more than one zero in any row or column of the correlation table.

## B. Four-zero classes

Using the freedom of relabeling, it is easy to see that there remain only two other kinds of four-zero correlation tables that are of interest:

Class 4a: All blocks have exactly one zero each (Table IVa)

Class 4b: Two non-neighboring blocks each contains two zeros that lie on the opposite corner (Table IVb)

Interestingly, Fritz already showed in Ref. [56] that correlations from Class 4a necessarily violate the NS conditions of Eq. (2), and are thus not quantum realizable. For Class 4b, we prove in Appendix B that all such  $\vec{P} \in \mathcal{Q}$  must be local. A

	x =	= 0	x =	= 1
	0	1	0	1
y = 0	0			
y = 0				0
y=1 0			0	
y-1		0		

(a) Class 4a: All four blocks have one zero each.

	x =	= 0	x =	= 1
	0	1	0	1
y=0	0			
y = 0		0		
y=1 0				
$\frac{g-1}{1}$				

(e) Class 2a: The two zeros appear in the same block at the (anti) diagonal positions.

	x =	= 0	x =	= 1
	0	1	0	1
y=0		0		
y = 0	0			
y=1				0
y=1			0	

(b) Class 4b: Two nonneighboring blocks have two DZs each.

	x =	= 0	x =	= 1
	0	1	0	1
y=0	0			
y = 0				0
y=1				
y-1				

(f) Class 2b: The two zeros appear in blocks with the same value of x (or y).

	x = 0		x = 1		
	0	1	0	1	
y = 0	0				
y = 0				0	
y=1 0					
y-1		0			

(c) Class 3a: Three blocks having one zero each.

	x = 0		x = 1		
	0	1	0	1	
y=0	0				
y = 0					
y=1				0	
y=1					

(g) Class 2c: The two zeros appear in non-neighboring blocks.

	<i>x</i> =	= 0	<i>x</i> =	= 1
	0	1	0	1
y = 0	0			
y = 0		0		
y=1 0				0
y-1				

(d) Class 3b: One block has two DZs, the remaining zero is in a non-neighboring block.

	x = 0		x = 1		
	0	1	0	1	
y=0	0				
y = 0					
y=1 0					
y=1					

(h) Class 1: There is only zero in the table.

Table IV: Modulo the freedom of relabeling, there are only eight distinct classes of correlation tables having four or fewer zeros. Classes having more than one zero in a row or column are omitted as they cannot contain nonlocal quantum correlations (see Lemma III.1.)

simple quantum example in this Class consists in measuring

$$A_0 = B_0 = \sigma_z, \quad A_1 = B_1 = \sigma_x,$$
 (19a)

on the Bell pair

$$|\Phi_2^+\rangle = \frac{1}{\sqrt{2}}(|0\rangle|0\rangle + |1\rangle|1\rangle),\tag{19b}$$

where  $\sigma_z$  and  $\sigma_x$  are Pauli matrices.

# C. Three-zero classes

The remaining possibilities of correlation tables with three zeros fall under—after an appropriate relabeling—two distinct classes:

Class 3a: Three blocks having one zero (Table IVc)

Class 3b: One block has two DZs (ADZs) and a non-neighboring block has another zero (Table IVd)

We define the sets of quantum correlations corresponding to these boundary classes as

$$Q_{3a} := \{ \vec{P} \mid \vec{P} \in \mathcal{Q}, \\ P(0,0|0,0) = P(1,1|1,0) = P(1,1|0,1) = 0 \}, \\ Q_{3b} := \{ \vec{P} \mid \vec{P} \in \mathcal{Q}, \\ P(0,0|0,0) = P(1,1|0,0) = P(1,0|1,1) = 0 \}.$$
(20)

#### 1. Class 3a

For Class 3a, there is a well-known quantum realization due to Hardy [36], which consists of

$$|\psi\rangle = \alpha(|0\rangle|1\rangle + |1\rangle|0\rangle) + \sqrt{1 - 2\alpha^2} \, |1\rangle|1\rangle \,, \tag{21a}$$

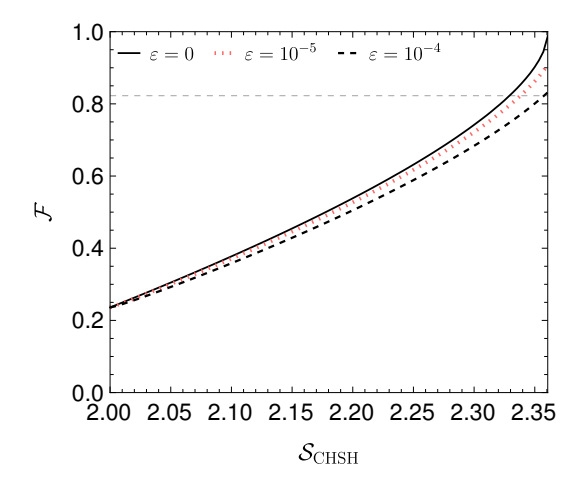
$$A_0 = B_0 = \sigma_z$$
,  $A_1 = B_1 = \mathbb{1}_2 - 2 |+\rangle \langle +|$ , (21b)

where 
$$\alpha=\sqrt{\frac{3-\sqrt{5}}{2}}$$
 and  $|+\rangle=\frac{1}{\sqrt{1-\alpha^2}}(\sqrt{1-2\alpha^2}\,|0\rangle-a\,|1\rangle.$ 

The resulting correlation  $\vec{P}_{Hardy} \in \mathcal{Q}_{3a}$  reads as:

$$\vec{P}_{\text{Hardy}} = \frac{\begin{vmatrix} x = 0 & x = 1 \\ 0 & 1 & 0 & 1 \\ y = 0 & 0 & \frac{1-\nu}{2} & \frac{1-3\nu}{2} & \nu \\ 1 & \frac{1-\nu}{2} & \nu & \frac{1+\nu}{2} & 0 \\ y = 1 & 0 & \frac{1-3\nu}{2} & \frac{1+\nu}{2} & \frac{1-3\nu}{2} & \frac{1+\nu}{2} & \frac{1-3\nu}{2} \\ 1 & \nu & 0 & \frac{1-3\nu}{2} & \frac{5\nu-1}{2} \end{vmatrix}}, \quad (22)$$

where  $\nu=\sqrt{5}-2$ . This particular correlation is known to be non-exposed [35] and provide a self-test [39] for the partially entangled two-qubit pure state of Eq. (21a). Moreover, from the result of [63], we know that for quantum correlations having exactly the zeros shown in Table IVc, its maximum achievable CHSH violation is  $\mathcal{S}_{\text{CHSH}}=10(\sqrt{5}-2)\approx 2.36068$ . The robustness of these self-testing results is illustrated in Fig. 1. More recently, a family of correlations from this class have been provided in [43]. Intriguingly, each correlation from this family again self-tests a partially entangled two-qubit state.



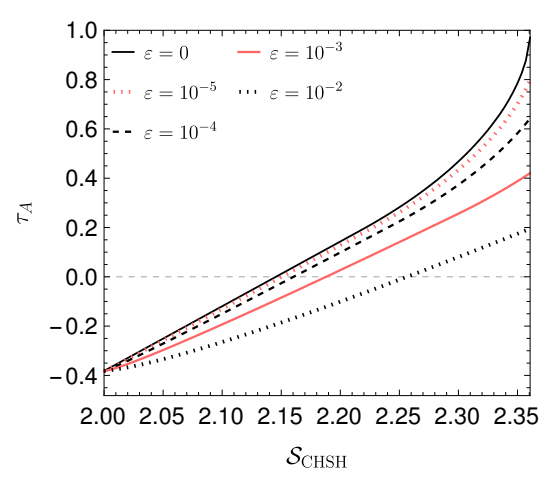


Figure 1: Plots illustrating the robustness of the self-testing result pertinent to the correlation  $\vec{P}_{\text{Hardy}}$  of Eq. (22) from Class 3a. The top and the lower plot show as a function of the Bell value  $S_{CHSH}$ , respectively, a lower bound on the relevant figure of merit for the self-testing of the two-qubit state of Eq. (21a) and the observables of Eq. (21b). Notice that due to the symmetry in Alice's and Bob's reference measurements, it suffices to show the plot for Alice. Here and below,  $\varepsilon$  represents the allowed deviation from the required zero probability ( $\mathcal{NS}$  boundary). Throughout, we use the level-3 outer approximation of Q due to [15] in the fidelity (top) plot but the level-4 outer approximation for the others. Each dashed line marks the respective value for the figure of merit achievable by a classical strategy, i.e., only the region above the horizontal line could give nontrivial self-testing. For details about these figures of merit, see Appendix C.

# 2. Class 3b

For Class 3b, an example quantum realization involves

$$|\psi\rangle = \cos\theta_0 |0\rangle |1\rangle + \sin\theta_0 |1\rangle |0\rangle, \qquad (23a)$$

and the dichotomic observables

$$A_0 = \sigma_z, \quad A_1 = \cos 2\alpha_0 \, \sigma_z - \sin 2\alpha_0 \, \sigma_x,$$
  

$$B_0 = \sigma_z, \quad B_1 = -\cos 2\beta_0 \, \sigma_z - \sin 2\beta_0 \, \sigma_x,$$
(23b)

where

$$\theta_0 = \tan^{-1} \frac{1}{3} \left( -1 - \frac{2}{\tau} + \tau \right), \quad \tau = \sqrt[3]{17 + 3\sqrt{33}}$$

$$\alpha_0 = \tan^{-1} \sqrt{\tan \theta}, \quad \beta_0 = \frac{\pi}{2} - \alpha_0.$$
(23c)

This quantum strategy can be self-tested using the resulting correlation (see Appendix D 2 for a proof):

$$\vec{P}_{Q} := \frac{\begin{vmatrix} x = 0 & x = 1 \\ 0 & 1 & 0 & 1 \\ y = 0 & 0 & 0 & \frac{1}{2} - \kappa_{2} & \kappa_{1} & \kappa_{3} \\ \frac{1}{2} + \kappa_{2} & 0 & \frac{1}{2} & \kappa_{2} \\ y = 1 & 0 & \kappa_{2} & \kappa_{3} & \frac{1}{2} - \kappa_{1} & 0 \\ 1 & \frac{1}{2} & \kappa_{1} & 2\kappa_{1} & \frac{1}{2} - \kappa_{1} \end{vmatrix}$$
(24a)

where

$$\kappa_{1} = \frac{1}{2} \left( \frac{\tau^{2} - \tau - 2}{2\tau} \right)^{3} \approx 0.0804,$$

$$\kappa_{2} = \frac{1 - \cos(2 \tan^{-1} \sqrt{\tan \theta_{0}})}{2 \sec^{2} \theta_{0}} \approx 0.2718,$$

$$\kappa_{3} = \frac{1 - 2\kappa_{1} - 2\kappa_{2}}{2}.$$
(24b)

The robustness of these self-testing results is illustrated in Fig. 2. The correlation of Eq. (24) is also provably non-exposed (see Appendix G 1).

In Appendix D1, we prove that among all quantum correlations having the zeros shown in Table IVd, the quantum strategy of Eq. (23) gives the maximal CHSH violation

$$S_{\text{CHSH}} = 4 - 4(2\kappa_1 + \kappa_2) \approx 2.26977.$$
 (25)

Before moving to other Classes with fewer zeros, we note that the non-exposed nature of  $\vec{P}_{\text{Hardy}}$  and  $\vec{P}_{\text{Q}}$  can be illustrated using a projection plot (see also Figure 5 of [35]). Fig. 3a and Fig. 3b show, respectively, a 2-dimensional projection plot of  $\mathcal{NS}$ ,  $\mathcal{L}$ , and an outer approximation of  $\mathcal{Q}$  (due to [15]) on a plane with its axes given by  $\mathcal{S}_{\text{CHSH}}$  and a linear sum of probabilities that are expected to vanish for the two Classes. For comparisons, we also mark on these plots the position of  $\vec{P}_{\text{PR}}$  [Eq. (14)], the relabeled ( $a=0 \leftrightarrow a=1$ ) version of  $\vec{P}_{\text{PR}}$  denoted by  $\vec{P}_{\text{PR},2}$ , and their noisy versions giving the maximal CHSH violation in quantum theory:

$$\vec{P}_{PR,2} \stackrel{a=0 \leftrightarrow a=1}{=} \vec{P}_{PR},$$

$$\vec{P}_{CHSH} = \frac{1}{\sqrt{2}} \vec{P}_{PR} + (1 - \frac{1}{\sqrt{2}}) \vec{P}_{\mathbb{I}},$$

$$\vec{P}_{CHSH,2} = \frac{1}{\sqrt{2}} \vec{P}_{PR,2} + (1 - \frac{1}{\sqrt{2}}) \vec{P}_{\mathbb{I}},$$
(26)

where  $\vec{P_{\mathbb{I}}}$  is the uniform distribution, i.e.,  $P_{\mathbb{I}}(a,b|x,y)=\frac{1}{4}$  for all a,b,x,y.

<sup>&</sup>lt;sup>2</sup> To determine the said outer approximation of the upper (lower) boundary of  $\mathcal Q$  on these plots, we compute, for each *fixed* value of the Bell function specified on the horizontal axis, the maximum (minimum) CHSH value over all  $\vec{P} \in \tilde{\mathcal Q}_\ell$  where  $\tilde{\mathcal Q}_\ell$  is the level- $\ell$  approximation of  $\mathcal Q$  due to [15].

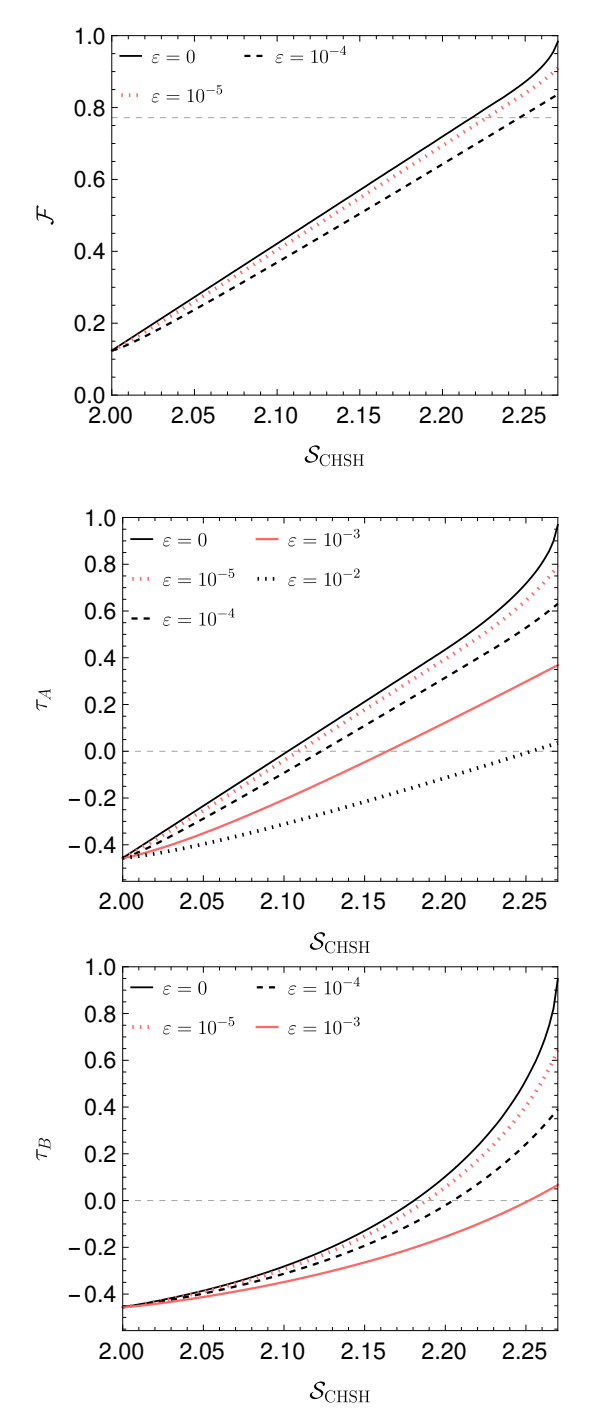
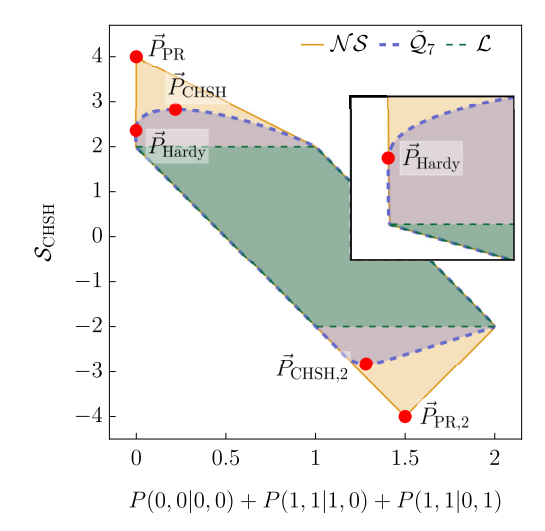
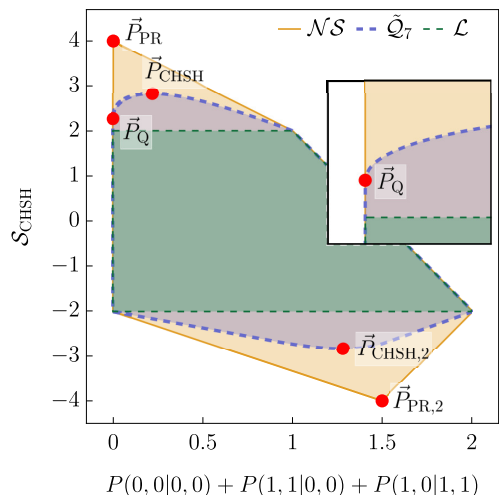


Figure 2: Plots illustrating the robustness of the self-testing result pertinent to the correlation  $\vec{P}_Q$  of Eq. (24) from Class 3b. The top, middle, and bottom plot show as a function of the Bell value  $\mathcal{S}_{\text{CHSH}}$ , respectively, a lower bound on the relevant figure of merit for the self-testing of the two-qubit state of Eq. (23a), the observables of Alice, and that of Bob [both specified in Eq. (23b)]. For the significance of  $\varepsilon$ , the dashed horizontal line, and other details related to the plots, see the caption of Fig. 1 and Appendix C.



(a) A projection plot illustrating  $\mathcal{Q}_{3a}$ , which consists of all quantum correlations satisfying P(0,0|0,0)+P(1,1|1,0)+P(1,1|0,1)=0. These correlations lie on the vertical line where the value of the horizontal axis is zero. Among them,  $\vec{P}_{\text{Hardy}}$  specified in Eq. (22) gives the maximal Bell violation.



(b) A projection plot illustrating  $\mathcal{Q}_{3b}$ , which consists of all quantum correlations satisfying P(0,0|0,0)+P(1,1|0,0)+P(1,0|1,1)=0. These correlations lie on the vertical line where the value of the horizontal axis is zero. Among them,  $\vec{P}_Q$  specified in Eq. (24b) gives the maximal Bell violation and is a self-test for the quantum strategy of Eq. (23).

Figure 3: Two-dimensional projections of  $\mathcal{NS}$ ,  $\mathcal{L}$ , and an outer approximation [15] of  $\mathcal{Q}$  onto the plane labeled by the CHSH value  $\mathcal{S}_{\text{CHSH}}$ , cf. Eq. (5), and some linear sum of probabilities. When the horizontal parameter is equal to zero, we recover the configurations specified, respectively, in the correlation tables of Table IVc and Table IVd. The insets illustrate, correspondingly, the non-exposed nature of both  $\vec{P}_{\text{Hardy}}$  and  $\vec{P}_{\text{Q}}$ . The explicit form of the other  $\vec{P}$ 's shown are given in Eq. (14) and Eq. (26).

## D. Classes having less then three zeros

By exploiting the freedom of relabeling, it is easy to see that there remain three two-zeros Classes and an one-zero Class that can be described as follows:

Class 2a: The are two DZs (or ADZs) in the same block (Table IVe)

Class 2b: The two zeros appear in two neighboring blocks having the same value of x (or y) (Table IVf)

Class 2c: The two zeros appear in two non-neighboring blocks (Table IVg)

Class 1: There is only one zero somewhere in the table (Table IVh)

Accordingly, the sets of quantum correlations exhibiting these structures of zeros are defined as

$$Q_{2a} := \{ \vec{P} \mid \vec{P} \in \{ \mathcal{Q} \setminus \mathcal{Q}_{3b} \}, \\ P(0,0|0,0) = P(1,1|0,0) = 0 \},$$

$$Q_{2b} := \{ \vec{P} \mid \vec{P} \in \{ \mathcal{Q} \setminus \mathcal{Q}_{3a} \}, \\ P(0,0|0,0) = P(1,1|1,0) = 0 \},$$

$$Q_{2c} := \{ \vec{P} \mid \vec{P} \in \{ \mathcal{Q} \setminus \{ \mathcal{Q}_{3a} \cup \mathcal{Q}_{3b} \} \}, \\ P(0,0|0,0) = P(1,0|1,1) = 0 \},$$

$$Q_{1} := \{ \vec{P} \mid \vec{P} \in \{ \mathcal{Q} \setminus \{ \mathcal{Q}_{3a} \cup \mathcal{Q}_{3b} \cup \mathcal{Q}_{2a} \cup \mathcal{Q}_{2b} \cup \mathcal{Q}_{2c} \} \}, \\ P(0,0|0,0) = 0 \}.$$

$$(27)$$

1. Class 2a

For Class 2a, a particular quantum realization makes use of the maximally entangled two-qubit state, cf. Eq. (19b), and the following observables

$$A_0 = \sigma_z, \quad A_1 = \cos 2\alpha \, \sigma_z + \sin 2\alpha \, \sigma_x, B_0 = -\sigma_z, \quad B_1 = \cos 2\beta \, \sigma_z + \sin 2\beta \, \sigma_x$$
 (28)

with  $\alpha = \frac{5\pi}{6}$  and  $\beta = \frac{2\pi}{3}$ . The corresponding correlation is

$$\vec{P}_{Q,2} := \frac{\begin{vmatrix} x = 0 & x = 1 \\ 0 & 1 & 0 & 1 \\ y = 0 & 0 & 0 & \frac{1}{2} & \frac{1}{8} & \frac{3}{8} \\ 1 & \frac{1}{2} & 0 & \frac{3}{8} & \frac{1}{8} \\ 1 & \frac{3}{8} & \frac{1}{8} & \frac{3}{8} & \frac{1}{8} \\ 1 & \frac{3}{8} & \frac{1}{8} & \frac{1}{8} & \frac{3}{8} \end{vmatrix}}, \tag{29}$$

giving the maximal CHSH value  $\mathcal{S}_{\text{CHSH}}=2.5$  among all  $\vec{P}\in\mathcal{Q}_{2a}$ . The proof is completely analogous to that given in Appendix D1 for  $\vec{P}\in\mathcal{Q}_{3b}$  and is thus omitted. Note that this correlation satisfies  $\langle A_0B_0\rangle=-1$ ,

 $\max\{|\langle A_1B_1\rangle, |\langle A_0B_1\rangle|, |\langle A_1B_0\rangle|\} < 1$ , and saturates the inequality:

$$2\langle A_1 B_1 \rangle \langle A_1 B_0 \rangle \langle A_0 B_1 \rangle + \langle A_1 B_1 \rangle^2 + \langle A_1 B_0 \rangle^2 + \langle A_0 B_1 \rangle^2 \le 1.$$
(30)

Hence [64] (see also the paragraphs below Eq. (23) of [35]), the two-zero nonlocal correlation  $\vec{P}_{Q,2}$  can be used to self-test [26] the above quantum strategy and is an extreme point. The robustness of these self-testing result is illustrated in Fig. 4. In Appendix G2, we further show that  $\vec{P}_{Q,2}$  is non-exposed.

## 2. Class 2b

For Class 2b, an explicit quantum realization is given by

$$|\psi\rangle = \frac{1}{\sqrt{2}}(\cos\alpha |0\rangle|1\rangle + |1\rangle|0\rangle - \sin\alpha |1\rangle|1\rangle),$$
 (31a)

$$A_0 = \sigma_z, \quad A_1 = \cos 2\alpha \, \sigma_z - \sin 2\alpha \, \sigma_x, B_0 = \sigma_z, \quad B_1 = \cos 2\beta \, \sigma_z - \sin 2\beta \, \sigma_x,$$
(31b)

where  $\alpha = \frac{\pi}{6}$  and  $\beta = \frac{\pi}{4}$ , thereby giving

$$\vec{P}_{Q,3} := \frac{\begin{vmatrix} x = 0 & x = 1 \\ 0 & 1 & 0 & 1 \end{vmatrix}}{y = 0 & 0 & 0 & \frac{1}{2} & \frac{1}{8} & \frac{3}{8} \\ 1 & \frac{3}{8} & \frac{1}{8} & \frac{1}{2} & 0 \end{vmatrix}} . \tag{32}$$
$$y = 1 & 0 & \frac{3}{16} & \frac{9}{16} & \frac{9}{16} & \frac{3}{16} \\ 1 & \frac{3}{16} & \frac{1}{16} & \frac{1}{16} & \frac{3}{16} \end{vmatrix}}$$

In Appendix E 1, we show that this correlation gives the maximal CHSH value of  $\mathcal{S}_{\text{CHSH}}=2.5$  among all  $\vec{P}\in\mathcal{Q}_{2b}$ .

Notice that a generalization of Hardy's argument [36] can be given [65] for nonlocal correlations in Class 2b using

$$P(0,0|0,0) = 0, P(1,1|1,0) = 0,$$
  
 $P(1,1|0,1) = q_1, P(1,1|1,1) = q_2,$  (33)

and a success probability defined by  $D=q_2-q_1$ . This argument has a different logical structure from the so-called Cabello's argument formulated in [41] (inspired by [66], see also [40]). In particular, it results in an even higher maximal success probability of D=0.125. Indeed, as with the results in [63], it is easy to verify that the CHSH violation and the success probability for  $\vec{P} \in \mathcal{Q}_{2b}$  is related linearly by  $\mathcal{S}_{\text{CHSH}}=4D+2$ . This implies that the maximal value of D can be achieved only by  $\vec{P}_{\text{Q},3}$ , which provides a self-test (see Appendix E2) for the quantum strategy given in Eq. (31). The robustness of these self-testing result is illustrated in Fig. 5. In Appendix G 3, we also show that  $\vec{P}_{\text{Q},3}$  is non-exposed. For the advantage of this nonlocality-without-inequality argument over the others, see [65] by some of the present authors.

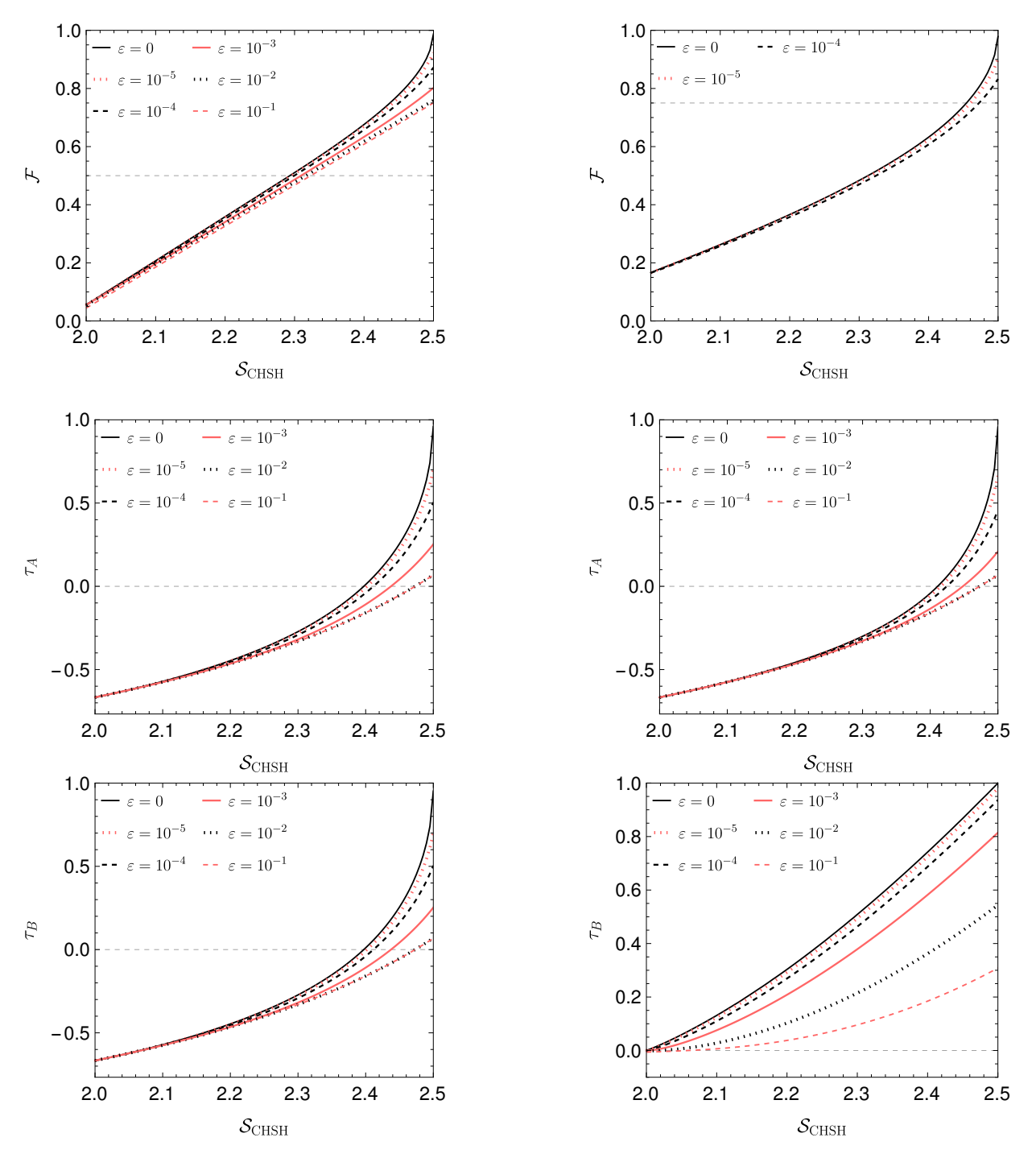


Figure 4: Plots illustrating the robustness of the self-testing result pertinent to the correlation  $\vec{P}_{Q,2}$  of Eq. (29) from Class 2a. The top, middle, and bottom plot show as a function of the Bell value  $S_{CHSH}$ , respectively, a lower bound on the relevant figure of merit for the self-testing of a Bell pair, the observables of Alice, and that of Bob [both specified in Eq. (28)]. For the significance of  $\varepsilon$ , the dashed horizontal line, and other details related to the plots, see the caption of Fig. 1 and Appendix C.

Figure 5: Plots illustrating the robustness of the self-testing result pertinent to the correlation  $\vec{P}_{Q,3}$  of Eq. (32) from Class 2b. The top, middle, and bottom plot show as a function of the Bell value  $S_{CHSH}$ , respectively, a lower bound on the relevant figure of merit for the self-testing of the two-qubit state of Eq. (31a), the observables of Alice, and that of Bob [both specified in Eq. (31b)]. For the significance of  $\varepsilon$ , the dashed horizontal line, and other details related to the plots, see the caption of Fig. 1 and Appendix C.

## 3. Class 2c

For Class 2c, the distribution of zeros coincide with that required for Cabello's argument. In this regard, it is known that the following quantum correlation [40] in  $Q_{2c}$ 

$$\vec{P}_{\text{Cabello}} \approx \frac{\begin{vmatrix} x = 0 & x = 1 \\ 0 & 1 & 0 & 1 \\ y = 0 & 0 & 0.2770 & 0.1444 & 0.1326 \\ 1 & 0.6410 & 0.0820 & 0.5786 & 0.1444 \\ y = 1 & 0 & 0.3068 & 0.3342 & 0.6410 & 0 \\ 1 & 0.3342 & 0.0247 & 0.0820 & 0.2770 \\ \end{vmatrix}$$
(34)

gives the maximal probability of success for this argument. Again, from [63], we know that this also gives the maximal CHSH violation of  $\mathcal{S}_{\text{CHSH}} \approx 2.4312$  among all  $\vec{P} \in \mathcal{Q}_{2c}$ .

The correlation  $\vec{P}_{\text{Cabello}}$  can be obtained using

$$|\psi\rangle=k_1\,|0\rangle|0\rangle+k_2\,|0\rangle|1\rangle+k_2\,|1\rangle|0\rangle)+k_3\,|1\rangle|1\rangle\,. \eqno(35a)$$

$$A_0 = -\sigma_z, \quad A_1 = -\cos 2\alpha \, \sigma_z + \sin 2\alpha \, \sigma_x, B_0 = \cos 2\alpha \, \sigma_z - \sin 2\alpha \, \sigma_x, \quad B_1 = -\sigma_z,$$
 (35b)

where

$$k_1 = \frac{1}{6} \left( 4 - \frac{\mu_1^2 + 1}{\mu_1} \right), \quad k_2 = \sqrt{1 - \frac{31\sqrt[3]{36}}{12\mu_2} + \frac{\sqrt[3]{6}\mu_2}{12}},$$
  
 $k_3 = \frac{1}{6} \left( \frac{\mu_3^2 - 29}{\mu_3} - 2 \right), \quad \alpha = \tan^{-1} \sqrt{\frac{\mu_1 + \mu_2 - 1}{12}},$ 

 $\mu_1=\sqrt[3]{53-6\sqrt{78}},~\mu_2=\sqrt[3]{67\sqrt{78}-414},~\mu_3=\sqrt[3]{307+39\sqrt{78}},~\mu_\pm=\sqrt[3]{359\pm12\sqrt{78}}.$  Recently,  $\vec{P}_{\rm Cabello}$  was shown [42] to self-test the partially entangled state of Eq. (35a). The robustness of these self-testing result is illustrated in Fig. 6. In Appendix G4 we further show that  $\vec{P}_{\rm Cabello}$  is non-exposed.

## 4. Class 1

For Class 1, a specific quantum realization is obtained from the symmetric state and measurements

$$|\psi\rangle = \sin\theta \left(\frac{|0\rangle|1\rangle + |1\rangle|0\rangle}{\sqrt{2}}\right) + \cos\theta |1\rangle|1\rangle, \quad (36a)$$

$$A_1 = B_1 = \sigma_z$$
,  $A_2 = B_2 = \cos \alpha \, \sigma_z + \sin \alpha \, \sigma_x$ , (36b)

where  $\theta = \cos^{-1}(\sqrt{\xi_2}) \approx 0.4267\pi$ ,  $\alpha = \cos^{-1}(\xi_1) \approx 0.4076\pi$ , while  $\xi_1 \approx 0.2862$ ,  $\xi_2 \approx 0.0521$ , and  $\xi_3 \approx 2.6353$  are, respectively, the smallest positive roots of the cubic polynomials:

$$p_1(x) = x^3 - 9x^2 - x + 1,$$
  

$$p_2(x) = 7x^3 - 35x^2 + 21x - 1,$$
  

$$p_3(x) = x^3 + 26x^2 - 36x - 104.$$
(37)

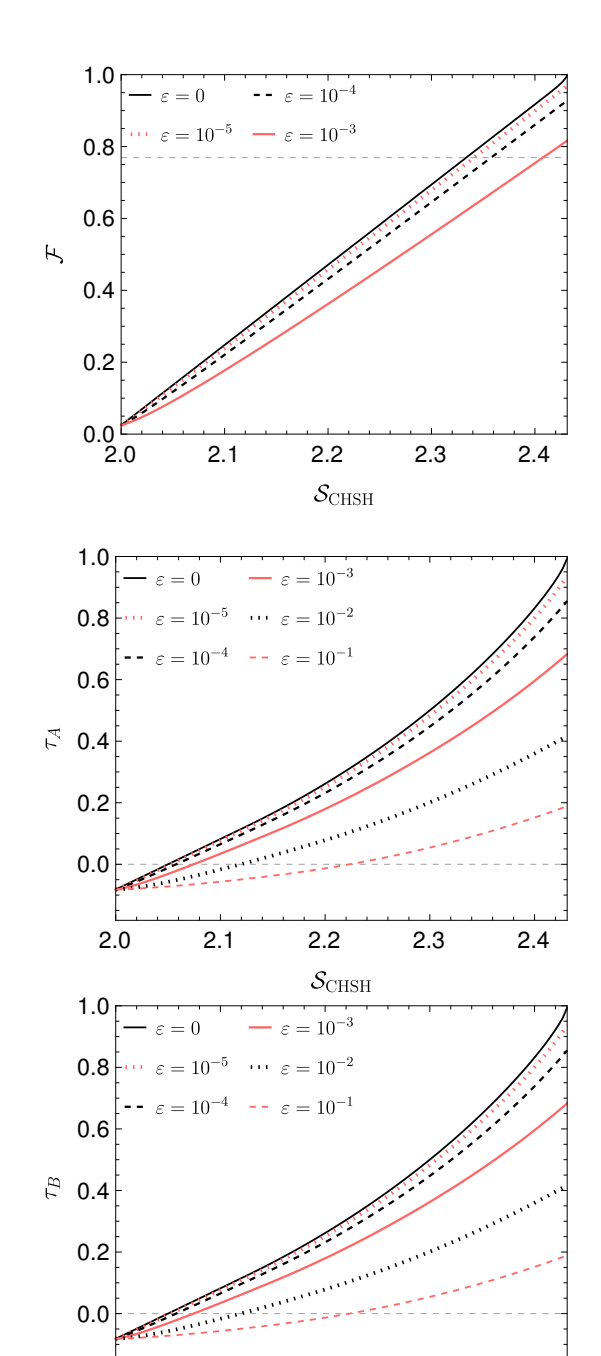


Figure 6: Plots illustrating the robustness of the self-testing result pertinent to the correlation  $\vec{P}_{\text{Cabello}}$  of Eq. (34) from Class 2c. The top, middle, and bottom plot show as a function of the Bell value  $\mathcal{S}_{\text{CHSH}}$ , respectively, a lower bound on the relevant figure of merit for the self-testing of the two-qubit state of Eq. (35a), the observables of Alice, and that of Bob [both specified in Eq. (35b)]. For the significance of  $\varepsilon$ , the dashed horizontal line, and other details related to the plots, see the caption of Fig. 1 and Appendix C.

2.2

 $\mathcal{S}_{ ext{CHSH}}$ 

2.3

2.4

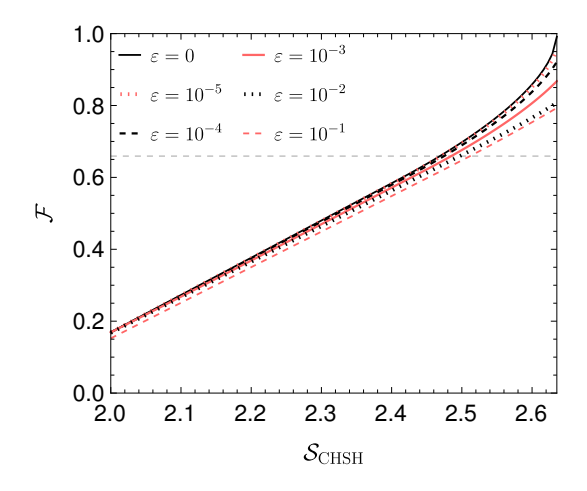
2.0

2.1

This quantum strategy gives the correlation

$$\vec{P}_{Q,4} \approx \frac{\begin{vmatrix} x = 0 & x = 1 \\ 0 & 1 & 0 & 1 \\ y = 0 & 0 & 0.4740 & 0.1692 & 0.3048 \\ 1 & 0.4740 & 0.0521 & 0.4740 & 0.0521 \\ y = 1 & 0 & 0.1692 & 0.4740 & 0.5492 & 0.0939 \\ 1 & 0.3048 & 0.0521 & 0.0939 & 0.2630 \end{vmatrix}, (38)$$

which provably gives the maximal CHSH violation of  $\mathcal{S}_{\text{CHSH}} = \xi_3$  among all  $\vec{P} \in \mathcal{Q}_1$ . In Appendix F, we prove that  $\vec{P}_{\text{Q},4}$  can be used to self-test the strategy of Eq. (36). The robustness of these self-testing results is shown in Fig. 7. In Appendix G 5, we show further that  $\vec{P}_{\text{Q},4}$  is non-exposed.



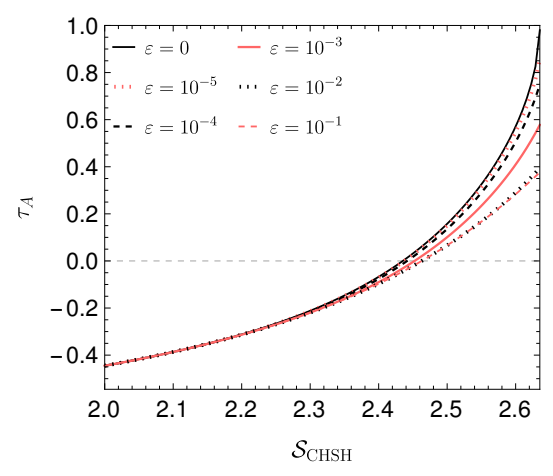


Figure 7: Plots illustrating the robustness of the self-testing result pertinent to the correlation  $\vec{P}_{Q,4}$  of Eq. (38) from Class 1. The top and bottom plot show as a function of the Bell value  $S_{\text{CHSH}}$ , respectively, a lower bound on the relevant figure of merit for the self-testing of the two-qubit state of Eq. (36a) and both parties' observables specified in Eq. (36b). Details about  $\varepsilon$  and these figures of merit can be found in Appendix C. For the significance of  $\varepsilon$ , the dashed horizontal line, and other details related to the plots, see the caption of Fig. 1 and Appendix C.

# IV. CORRELATIONS FROM FINITE-DIMENSIONAL MAXIMALLY ENTANGLED STATES

Consider now  $\mathcal{M}$ , the subset of  $\mathcal{Q}$  due to finite-dimensional maximally entangled states  $\{|\Phi_d^+\rangle\}_{d=2,3,\ldots}$ , see Section II A. To understand when the boundary of  $\mathcal{M}$  meets the boundary of  $\mathcal{NS}$ , we first derive the analog of Fact II.2 for  $\mathcal{M}$ .

**Lemma IV.1.** In the CHSH Bell scenario, all extreme points of  $\mathcal{M}$  are achievable by measuring a two-qubit maximally entangled states with projective measurements.

*Proof.* Let us begin by simplifying the notation and denote the POVM elements of Alice and Bob, respectively, by  $\{E_{a|x}\}_{a,x=0,1}$  and  $\{F_{b|y}\}_{b,y=0,1}$ . Then as mentioned in Eq. (8), the correlation due to the maximally entangled two-qudit state  $|\Phi_d^+\rangle$  can be written as

$$P(a,b|x,y) = \langle \Phi_d^+ | E_{a|x} \otimes F_{b|y} | \Phi_d^+ \rangle = \frac{\text{tr}(E_{a|x}^{\mathsf{T}} F_{b|y})}{d}.$$
(39)

Since we are concerned with a two-outcome Bell scenario, it follows from Theorem 5.4 of [67] (see also [68]) that it suffices to consider projective measurements for correlations  $\vec{P}$  lying on the boundary of  $\mathcal{M}$ . Moreover, by the Lemma of [55], there exists a local orthonormal basis such that all four projectors  $\{E_{a|x}\}_{a,x=0,1}$  are simultaneously block diagonal, with blocks of size  $2\times 2$  or  $1\times 1$ , i.e., <sup>3</sup>

$$E_{a|x}^{\mathsf{T}} = \bigoplus_{i=1}^{\frac{d+k}{2}} \Pi_i E_{a|x}^{\mathsf{T}} \Pi_i \quad \forall \ a, x = 0, 1$$
 (40)

where  $\Pi_i$  is the projection operator onto the *i*-th block and k  $(\frac{d-k}{2})$  is the number of  $1 \times 1$   $(2 \times 2)$  blocks.

Using Eq. (40) in Eq. (39) and the fact that the block projection operator satisfies  $(\Pi_i)^2 = \Pi_i$ , we get

$$P(a, b|x, y) = \frac{1}{d} \operatorname{tr} \left( \bigoplus_{i=1}^{\frac{d+k}{2}} \Pi_i E_{a|x}^{\mathsf{T}} \Pi_i F_{b|y} \right)$$

$$= \frac{1}{d} \sum_{i=1}^{\frac{d+k}{2}} \operatorname{tr} (\Pi_i E_{a|x}^{\mathsf{T}} \Pi_i F_{b|y})$$

$$= \sum_{i=1}^{\frac{d+k}{2}} \frac{2}{d} \frac{1}{2} \operatorname{tr} (E_{a|x}^{(i)\mathsf{T}} F_{b|y}^{(i)})$$
(41)

where  $E_{a|x}^{(i) \text{ T}} := \Pi_i E_{a|x}^{\text{ T}} \Pi_i$  and  $F_{b|y}^{(i)} := \Pi_i F_{b|y} \Pi_i$  are easily seen to define d-dimensional POVMs, with d=1 or 2.

Whenever  $\Pi_i$  projects onto a two-dimensional subspace,

$$\frac{1}{2} \operatorname{tr}(E_{a|x}^{(i)\mathsf{T}} F_{b|y}^{(i)}) = \langle \Phi_2^+ | E_{a|x}^{(i)} \otimes F_{b|y}^{(i)} | \Phi_2^+ \rangle \tag{42}$$

 $<sup>^3</sup>$  Here and below, we use the direct sum symbol  $\oplus$  to emphasize the block diagonal structure of the corresponding operators. Strictly,  $\oplus$  should be replaced by a regular sum  $\sum$  and each  $\Pi_i$ ,  $E_{a|x}^{\ T}$ ,  $F_{b|y}$ ,  $E_{a|x}^{(i)\ T}$ ,  $F_{b|y}^{(i)}$  should be thought of as a full d-dimensional matrix.

is a correlation in  $\mathcal{M}_2$  attainable by a two-qubit maximally entangled  $|\Phi_2^+\rangle$  using local POVM  $\{E_{a|x}^{(i)}\}$  and  $\{F_{b|y}^{(i)}\}$ . If instead,  $\Pi_i$  is a one-dimensional projector, the corresponding  $E_{a|x}^{(i)}$  and  $F_{b|y}^{(i)}$  are real numbers lying in [0,1], so as the expression  $\operatorname{tr}(E_{a|x}^{(i)}^{T}F_{b|y}^{(i)})$ . The latter can again be reproduced using  $|\Phi_2^+\rangle$  and POVM elements that are proportional to the identity operator. To complete the proof, we recall from [69] that for qubit measurements, all extremal POVMs are projectors. All in all, we thus see that *any* correlation in  $\mathcal M$  can always be written as a convex mixture of correlations attainable by performing projective measurements on  $|\Phi_2^+\rangle$ . In other words, extreme points of  $\mathcal M$  in this Bell scenario originate from performing projective measurements on  $|\Phi_2^+\rangle$ .

**Corollary IV.2.** In the CHSH Bell scenario, any  $\vec{P} \in \mathcal{M}_d$  obtained by performing projective measurements on  $|\Phi_d^+\rangle$  has a convex decomposition using at most  $\frac{d-1}{2}$  nonlocal  $\vec{P}' \in \mathcal{M}_2$  when d is odd, but  $\frac{d}{2}$  nonlocal  $\vec{P}' \in \mathcal{M}_2$  when d is even.

*Proof.* From the proof of Lemma IV.1, we see that any  $\vec{P} \in \mathcal{M}_d$  obtained by performing projective measurements on  $|\Phi_d^+\rangle$  admits the decomposition:

$$\vec{P} = \frac{2}{d} \sum_{i=1}^{\frac{d-k}{2}} \vec{P}'_i + \frac{1}{d} \sum_{j=1}^{k} \vec{P}''_j$$
 (43)

where k is the number of  $1 \times 1$  block in the decomposition of  $\{E_{a|x}^{\mathsf{T}}\}_{a,x=0,1}, \vec{P}'_i \in \mathcal{M}_2$  for all i, and  $\vec{P}''_j \in \mathcal{L}$  for all j. Clearly, only the  $\vec{P}'_i$  can be nonlocal. To complete the proof, note that for d odd,  $k \geq 1$  whereas for d even,  $k \geq 0$ .

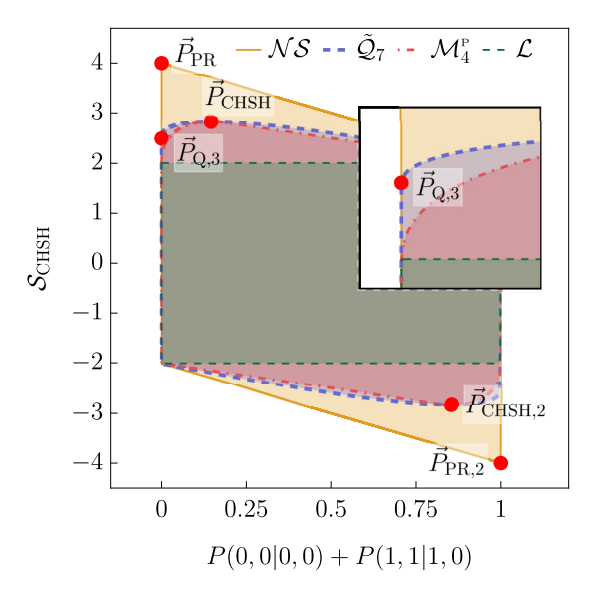
Using Lemma IV.1, one can show also the following corollary concerning the maximal CHSH violation by  $|\Phi_d^+\rangle$  (see Appendix H for a proof).

**Corollary IV.3.** The maximal CHSH violation by the maximally entangled two-qudit state  $|\Phi_d^+\rangle$  is:

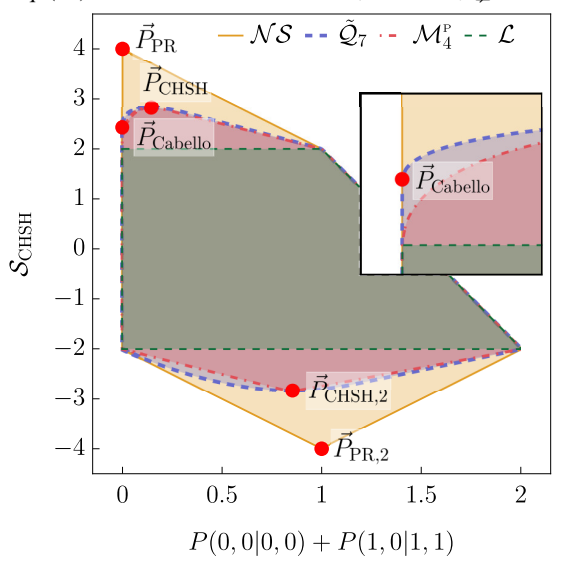
$$\mathcal{S}_{\text{CHSH}}^{\max}(|\Phi_d^+\rangle) = \begin{cases} 2\sqrt{2} \left(\frac{d-1}{d}\right) + \frac{2}{d}, & d = odd \\ 2\sqrt{2}, & d = even. \end{cases}$$
(44)

We now return to the problem of characterizing when the boundaries of  $\mathcal{M}$  meet the boundaries of  $\mathcal{NS}$ . For general quantum correlations, Classes shown in Table IV with three or fewer zeros are the only ones lying on the  $\mathcal{NS}$  boundary yet being outside the Bell polytope  $\mathcal{L}$ . Since  $\mathcal{M} \subsetneq \mathcal{Q}$ , these are the only boundary Classes that we need to consider for the present purpose. In Section III D 1, we give an example of a nonlocal correlation in  $\mathcal{Q}_{2a}$  due to  $|\Phi_2^+\rangle$ , thus showing that the overlap of  $\mathcal{M}$  with  $\mathcal{NS}$  in Class 2a is not empty. The following theorem, which we show below, takes care of most of the other Classes.

**Theorem IV.4.** Nonlocal correlation in  $Q_{2b}$  and  $Q_{2c}$  (and hence, respectively,  $Q_{3a}$  and  $Q_{3b}$ ) cannot arise from any finite-dimensional maximally entangled state.



(a) A projection revealing the gap between  $\mathcal{Q}$  and  $\mathcal{M}$  within Class 2b, i.e., all correlations satisfying P(0,0|0,0)+P(1,1|1,0)=0 (shown on the vertical line where the value of the horizontal axis is zero). Among them,  $\vec{P}_{Q,3}$  of Eq. (32) gives the maximal  $S_{\text{CHSH}}$  value and is a self-test for the quantum strategy of Eq. (31). As shown in Theorem IV.4,  $\mathcal{M} \cap \mathcal{Q}_{2b} \subsetneq \mathcal{L}$ .



(b) A projection revealing the gap between  $\mathcal{Q}$  and  $\mathcal{M}$  within Class 2c, i.e., all correlations satisfying P(0,0|0,0)+P(1,0|1,1)=0 (shown on the vertical line where the value of the horizontal axis is zero). Among them,  $\vec{P}_{\text{Cabello}}$  of Eq. (34) gives the maximal  $\mathcal{S}_{\text{CHSH}}$  value and is a self-test for the quantum strategy of Eq. (35). As shown in Theorem IV.4,  $\mathcal{M} \cap \mathcal{Q}_{2c} \subsetneq \mathcal{L}$ .

Figure 8: Two-dimensional projection of  $\mathcal{NS}$ ,  $\mathcal{L}$ ,  $\mathcal{Q}_7$ , and  $\mathcal{M}_4^P$  onto the plane labeled by the CHSH Bell value  $\mathcal{S}_{\text{CHSH}}$  and some linear sum of probabilities (see text for details). When the horizontal parameter is equal to zero, we recover the configuration specified in the correlation tables of Table IVf and Table IVf. The insets clearly illustrate, correspondingly, the non-exposed nature of both  $\vec{P}_{Q,3}$  and  $\vec{P}_{\text{Cabello}}$  as well as the gap between  $\mathcal{Q}$  and  $\mathcal{M}$  within each Class. The explicit form of the other  $\vec{P}$ 's shown are given in Eq. (14) and Eq. (26).

*Proof.* To prove the Theorem, we make use of the following Lemma, whose proof is given in Appendix I.

**Lemma IV.5.** For the maximally entangled state  $|\Phi_d^+\rangle$ , if the probability  $P(a,b|x,y) = \langle \Phi_d^+|E_{a|x} \otimes F_{b|y} | \Phi_d^+\rangle = 0$  for any  $x,y,a,b \in \{0,1\}$ , the corresponding operators  $E_{a|x}^{T}$  and  $F_{b|y}$  can be diagonalized in the same basis.

Since extremal correlations of  $\mathcal{M}$  have qubit realization, cf. Lemma IV.1, it suffices to show that  $|\Phi_2^+\rangle$  cannot give nonlocal correlation in these Classes. Moreover, one should bear in mind that (i) correlations having less zeros may be obtained as mixtures of correlations having more zeros, but not the other way around (ii)  $\vec{P} \in \mathcal{Q}$  (and hence  $\mathcal{M}$ ) having more than three zeros must be local (iii) it suffices to consider rank-one projective measurements if we want the resulting extremal correlation to be nonlocal.

Now, note from Lemma IV.5 that for rank-one projective measurements acting on  $|\Phi_2^+\rangle$ ,

$$P(0,0|0,0) = 0 \implies P(1,1|0,0) = 0,$$
 (45a)

$$P(1,0|1,1) = 0 \implies P(0,1|1,1) = 0$$
 (45b)

Applying Eq. (45a) to correlations from Class 3a (Table IVc), we end up having two zeros on the same row of the correlation table. By Lemma III.1, we know that such correlations must be local. Moreover, by point (i) and (ii) above, there cannot be mixtures of nonlocal correlations with more zeros that give a nonlocal  $\vec{P} \in \mathcal{M} \cap \mathcal{Q}_{3a}$ . Hence, all  $\vec{P} \in \mathcal{M} \cap \mathcal{Q}_{3a}$  are local. Similarly, applying Eq. (45a) to correlations in Class 2b (Table IVf) leads to correlations that are local since they have two zeros in the same row. Even though correlations from the Class 3a can be mixed to give correlations from the Class 2b, using the just-established result for  $\vec{P} \in \mathcal{M} \cap \mathcal{Q}_{3a}$ , we know that such mixtures must again be local.

Next, by applying Eq. (45b) to correlations in the Class 3b (Table IVd), we end up with correlations (up to relabeling) from the Class 4b (Table IVb). However, we already show in Appendix B that all  $\vec{P} \in \mathcal{Q}_{4b}$  are local. Together with point (i) and (ii) given above, we thus conclude that all  $\vec{P} \in \mathcal{M} \cap \mathcal{Q}_{3b}$  must be local. Finally, the application of Eq. (45a) to correlations in the Class 2c (Table IVg) give correlations in the Class 3b. Moreover, an inspection of Table IV shows that there are no other Classes of correlations that can be mixed to give correlations from the Class 2c. Hence, all  $\vec{P} \in \mathcal{M} \cap \mathcal{Q}_{2c}$  are local, which completes the proof of the Theorem.

Theorem IV.4 can be seen as a no-go theorem for self-testing maximally entangled states on the common boundaries of  $\mathcal Q$  and  $\mathcal N\mathcal S$  belonging to the aforementioned Classes. In a way, the theorem is anticipated given Lemma IV.1 and the absence [36, 40] of Hardy-type argument for the Bell state  $|\Phi_2^+\rangle$ . To illustrate the fact that  $\mathcal Q_{2b}\cap\mathcal M\subsetneq\mathcal L$  and  $\mathcal Q_{2c}\cap\mathcal M\subsetneq\mathcal L$ , we plot in Fig. 8a and 8b, correspondingly, the 2-dimensional projections of  $\mathcal N\mathcal S$ ,  $\mathcal L$ ,  $\tilde{\mathcal Q}_7$  (the level-7 outer approximation of  $\mathcal Q$  due to [15]) and  $\mathcal M_4$  (the level-4 outer approximation of

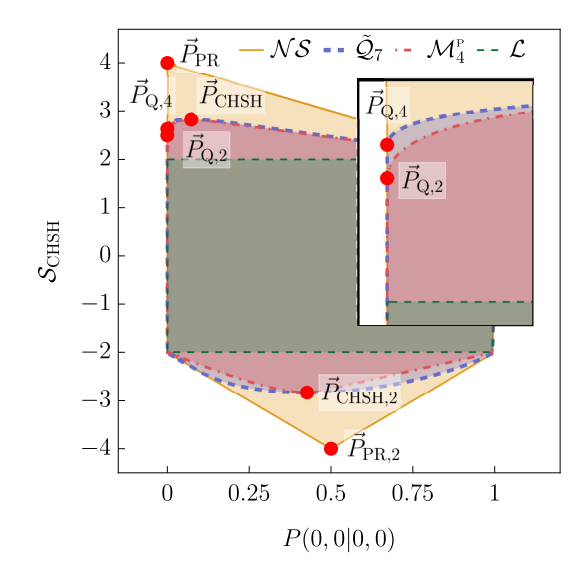


Figure 9: Two-dimensional projection of  $\mathcal{NS}$ ,  $\mathcal{L}$ ,  $\mathcal{Q}_7$ , and  $\mathcal{M}_4^{\mathsf{P}}$  onto the plane labeled by the CHSH value  $\mathcal{S}_{\text{CHSH}}$  and P(0,0|0,0). When the horizontal parameter is equal to zero, we recover the configuration specified in Table IVh. The inset clearly illustrates the gap between  $\mathcal{Q}$  and  $\mathcal{M}$  within Class 1 (i.e., when the horizontal value is zero) even though there exists nonlocal point  $\vec{P} \in \{\mathcal{Q}_1 \cap \mathcal{M}\}$  that is arbitrarily close to  $\vec{P}_{\mathbf{Q},2}$ . The explicit form of the other  $\vec{P}$ 's shown are given in Eq. (14) and Eq. (26).

 $\mathcal{M}$  due to [51]<sup>4</sup>). Indeed, in both cases, as the boundary of (this outer approximation of)  $\mathcal{M}$  approaches the boundary of  $\mathcal{NS}$ , it also approaches the boundary of  $\mathcal{L}$ .

What about Class 1? From the proof of Theorem IV.4 given above, we already see that with rank-one projective measurements acting on  $|\Phi_2^+\rangle$ ,  $P(0,0|0,0)=0 \Longrightarrow P(1,1|0,0)=0$ , therefore such quantum strategies cannot generate  $\vec{P}\in\mathcal{M}\cap\mathcal{Q}_1$ . In turn, when combined with Corollary IV.2, we come to the intriguing observation that  $\vec{P}\in\mathcal{M}\cap\mathcal{Q}_1$  are non-extremal in  $\mathcal{M}$ . However, if we introduce some noise to Alice's 0-th measurements in Eq. (28), namely, by adopting for some positive  $\epsilon\approx0$ ,

$$M_{0|0}^A = (1 - \epsilon) \frac{\mathbb{1}_2 + A_0}{2}$$
 and  $M_{1|0}^A = \mathbb{1}_2 - M_{0|0}^A$  (46)

instead of Eq. (11), it is clear that we can generate nonlocal  $\vec{P} \in \mathcal{M} \cap \mathcal{Q}_1$ . Moreover, it is easy to see that for such strategies,  $\sup_{0 < \epsilon < 1} \mathcal{S}_{\text{CHSH}} = 2.5$ , i.e., we can find  $\vec{P} \in \{\mathcal{Q}_1 \cap \mathcal{M}\}$  that is arbitrarily close to  $\vec{P}_{\mathbf{Q},2}$ . In fact, using the technique described in [51], we find that 2.5 matches the best upper bound on  $\mathcal{S}_{\text{CHSH}}$  for  $\vec{P} \in \mathcal{M} \cap \mathcal{Q}_1$  to within a numerical precision better than  $10^{-5}$ . Still, it is worth noting that this largest value

<sup>&</sup>lt;sup>4</sup> Strictly, the technique of [51] only outer approximates the set of M assuming projective measurements. However, as we remark in the proof of Theorem IV.4, M<sup>P</sup> and M coincide in this simplest Bell scenario.

Class	Necessarily $\in \mathcal{L}$ ?	$\mathcal{L}^c\cap\mathcal{M}\neq\emptyset?$	Quantum example $ \psi\rangle$	Extremal in Q?	Self-test?	Non-Exposed?	$\mathcal{S}_{ ext{CHSH}}^{ ext{max}}$	$E( \psi\rangle)$
4b (Table IVb)	Yes	N/A	Eq. (19)	No	No	No	2	1
3a (Table IVc)	No	No	Eq. (21) [36]	Yes	Yes [39]	Yes [35]	2.3607	0.6742
3b (Table IVd)	No	No	Eq. (23)	Yes	Yes	Yes	2.2698	0.7748
2a (Table IVe)	No	Yes	Eq. (28)	Yes	Yes	Yes	2.5	1
2b (Table IVf)	No	No	Eq. (31)	Yes	Yes	Yes	2.5	0.8113
2c (Table IVg)	No	No	Eq. (35) [40]	Yes	Yes [42]	Yes	2.4312	0.7794
1 (Table IVh)	No	Yes	Eq. (36)	Yes	Yes	Yes	2.6353	0.9255

Table V: Summary of our findings regarding the common boundaries of  $\mathcal Q$  and  $\mathcal N\mathcal S$ . These boundaries are classified according to the number of zeros present in the respective correlation tables, see Table IV. For each of these Classes given in the leftmost column, we list in the second and third column, respectively, whether a  $\vec{P} \in \mathcal Q$  from the Class is necessarily local and whether a nonlocal  $\vec{P} \in \mathcal Q$  from the Class can be realized using a finite-dimensional maximally entangled state (here  $\mathcal L^c$  denotes the complement of  $\mathcal L$  in  $\mathcal N\mathcal S$ , i.e., the set of nonlocal correlations). Further to the right, we give the equation number for the explicit quantum strategy realizing an example from this Class, whether the example is extremal in  $\mathcal Q$ , is a self-test, and is non-exposed. In the last two columns, we give, respectively, the maximal CHSH value attainable in each Class and the entanglement of formation [70]  $E(|\psi\rangle)$  of the state  $|\psi\rangle$  giving this maximum. Notice that even among those classes having the same number of zeros, the state  $|\psi\rangle$  giving a larger  $\mathcal S_{\text{CHSH}}^{\text{max}}$  may not have a larger amount of entanglement.

 $\mathcal{S}_{\text{CHSH}}$  that  $\vec{P} \in \mathcal{M}$  can approach within Class 1 lies strictly below the value of  $\mathcal{S}_{\text{CHSH}} \approx 2.63533$  attainable by  $\vec{P}_{\text{Q,4}} \in \mathcal{Q}_1$ , as illustrated in the inset of Fig. 9.

As a side remark, note that the mixing strategy given above allows one to transform quantum correlations belonging to one class to another class having fewer zeros.

#### V. CONCLUSION

Knowing when the boundary of the quantum set  $\mathcal{Q}$  meets the boundary of the no-signaling set  $\mathcal{NS}$  helps us better understand the limits of quantum resources when it comes to information processing tasks. In this work, we provide—independent of [38]—the complete characterization of when the boundary of these two sets meet in the simplest Bell scenario. Inspired by the work of [56], we classify the distinct cases—modulo relabeling—according the numbers of zero present in the correlation table (see Table IV). Our findings are summarized in Table V.

In addition to showing that only six of these Classes contain nonlocal correlations (also shown independently in [38]), we prove that only two of them contain nonlocal correlations that can be obtained using finite-dimensional maximally entangled states. For each of these Classes, we further determine the maximal possible CHSH-Bell-inequality violation and provide the quantum strategy leading to this maximum. Interestingly, all these quantum strategies can be self-tested by the resulting correlation with some level of robustness. Moreover, all these self-testing correlations are provably nonexposed [35].

In arriving at the above results, we obtain several other results that may be of independent interests. For example, we

establish in Theorem II.4 that in the CHSH Bell scenario, if all qubit strategies giving the same extremal quantum correlation are local-unitarily equivalent, then this correlation is a self-test. We also show in Corollary IV.2 that in this simplest Bell scenario, the set of correlations attainable by finite-dimensional maximally entangled states can be reproduced using mixtures of correlations attainable by a Bell pair in conjunction with projective measurements. In turn, this allows us to derive, among others, the maximal CHSH Bell inequality violation by an arbitrary finite-dimensional maximally entangled state, see Corollary IV.3.

An observant reader has probably noticed that the self-testing results that we have presented here for Class 3a, 3b, 2b, and 2c do not seem to be particularly robust. Thus, an obvious avenue of research is to see if the techniques of [71] can be adapted here to improve the robustness of these results. In fact, these results (and [72]) would suggest that the weak form [52, 53] of self-testing discovered in other Bell scenarios may well be absent in this Bell scenario. Another closely related question concerns the possibility to self-test other quantum correlations from the same Class. The recent work by Rai et al. [43] shows that this is possible for a four-parameter family of correlations from Class 3a. What about other classes?

Also worth noting is that among the correlations given in [43], our calculation based on  $21^4=194,481$  uniformly chosen samples show that, to a precision better than  $10^{-13}$ , all these self-testing Hardy-type correlations are non-exposed. Based on these observations, it seems conceivable that (1) all extremal quantum correlations on the boundary of  $\mathcal{NS}$  may be self-tested, and (2) all these self-testing correlations on the boundary of  $\mathcal{NS}$  are non-exposed. However, determining the validity of these conjectures in this or other more complicated Bell scenarios (see, e.g., [73]) clearly requires more work and shall thus be left for future work.

<sup>&</sup>lt;sup>a</sup> Although it was only shown in [39] and [42] that the quantum correlation self-tests the corresponding state, one can easily check there exists local unitaries  $(u_A=u_B=e^{i\theta}\oplus 1 \text{ for the state} \text{ and the measurements in Lemma.2 in [39] and } u_A=e^{i\phi}\oplus 1, u_B=e^{i\xi}\oplus 1 \text{ for Eq.(5) and Eq.(7) in [42])}$  such that Definition II.3 holds, and thus Theorem II.4 can be applied to also self-test the underlying measurements.

## ACKNOWLEDGMENTS

We are grateful to R. Augusiak, J. Kaniewski, and V. Scarani for helpful discussions, to A. Rai for helpful comments on an earlier version of this manuscript, to P.-S. Lin for sharing his code and other contributions to this research project. This work is supported by the National Science and Technology Council (formerly Ministry of Science and Technology), Taiwan (Grants No. 107-2112-M-006-005-MY2, 109-2112-M-006-010-MY3, MOST 110-2112-M-032-005-MY3, and MOST 111-2119-M-008-002), a grant provided by Academia Sinica through the Academia Sinica Research Award for Junior Research Investigators, and the Foundation for Polish Science through the First Team project (First TEAM/2017-4/31) co-financed by the European Union under the European Regional Development Fund.

#### Appendix A: Proof of Theorem II.4

The following proof mirrors that given in [39] for showing that the quantum correlation giving the maximal success probability in the original Hardy paradox [36] is a self-test.

*Proof.* Let us denote by  $\vec{P}$  the extremal nonlocal correlation of interest. By Neumark's theorem [46], all possible quantum strategies leading to  $\vec{P}$  can be realized using a pure entangled state (possibly of a higher Hilbert space dimension) and projective measurements. Then, by the Lemma shown in [55], there exists a local basis such that all the projective POVM elements on Alice's (Bob's) side are simultaneously block diagonal, with blocks of size  $2 \times 2$  or  $1 \times 1$ , i.e.,

$$\begin{split} M_{a|x}^A &= \bigoplus_i M_{a|x}^{A_i} = \bigoplus_i \Pi_i^A M_{a|x}^{A_i} \Pi_i^A, \\ M_{b|y}^B &= \bigoplus_j M_{b|y}^{B_j} = \bigoplus_j \Pi_j^B M_{b|y}^{B_j} \Pi_j^B, \end{split} \tag{A1}$$

where i, j are labels for the block and  $\Pi_i^A$  ( $\Pi_i^B$ ) is the projector onto the *i*-th (*j*-th) block of Alice's (Bob's) Hilbert space, in the sense that  $\bigoplus_i \Pi_i^A = \mathbb{1}_A$  and  $\bigoplus_j \Pi_j^B = \mathbb{1}_B$ . Using this in Born's rule, Eq. (6), we get

$$P(a, b|x, y) = \operatorname{tr}[\rho(M_{a|x}^{A} \otimes M_{b|y}^{B})]$$

$$= \operatorname{tr}\left[\rho \bigoplus_{i} M_{a|x}^{A_{i}} \otimes \bigoplus_{j} M_{b|y}^{B_{j}}\right]$$

$$= \sum_{i,j} \nu_{ij} \operatorname{tr}[\rho_{ij}(M_{a|x}^{A_{i}} \otimes M_{b|y}^{B_{j}})],$$

$$= \sum_{i,j} \nu_{ij} P_{ij}(a, b|x, y), \tag{A2}$$

where  $\nu_{ij} := \operatorname{tr}[\Pi_i^A \otimes \Pi_i^B) \rho(\Pi_i^A \otimes \Pi_i^B)]$  and when  $\nu_{ij} \neq 0$ ,

$$\rho_{ij} := \frac{(\Pi_i^A \otimes \Pi_j^B) \rho(\Pi_i^A \otimes \Pi_j^B)}{\nu_{ij}},$$

$$P_{ij}(a, b|x, y) := \operatorname{tr}[\rho_{ij}(M_{a|x}^{A_i} \otimes M_{b|y}^{B_j})].$$
(A3)

Note that the probability of a successful projection onto the *i*-th block of Alice's Hilbert space and the *j*-th block of Bob's Hilbert space can be factorized into the product of a successful projection onto the individual block of the respective Hilbert space, i.e.,  $\nu_{ij} = r_i s_j$ , where  $r_i = \operatorname{tr}[\Pi_i^A \operatorname{tr}_B(\rho) \Pi_i^A], s_j = \operatorname{tr}[\Pi_j^B \operatorname{tr}_A(\rho) \Pi_j^B] \geq 0$ , and  $\sum_i r_i = \sum_j s_j = 1$ .

By assumption,  $\vec{P}$  is extremal. However, we also see in Eq. (A2) that  $\vec{P}$  is a convex mixture of  $\vec{P}_{ij}$ . This can only hold if  $\vec{P}_{ij}$  is in fact  $\vec{P}$  for all i,j. This implies that  $\nu_{ij}$  involving one-dimensional projection must vanish as the otherwise surviving  $\rho_{ij}$  cannot lead to a nonlocal  $P_{ij}$ . Moreover, since the surviving local blocks are all of size  $2 \times 2$ , we know by assumption that for all i,j, the quantum strategy of  $\left\{ {{\rho _{ij}} = \left| {{\psi _{ij}}} \right\rangle \!\! \left\langle {{\psi _{ij}}} \right|,\{ M_{a|x}^{{A_i}}\},\{ M_{b|y}^{{B_j}}\}} \right\}$  is 2-equivalent to the reference strategy. In other words, there exist local unitaries  $u_{A,i}$  and  $u_{B,i}$ , cf. Eq. (13), such that

$$u_{A,i} \otimes u_{B,j} | \psi_{ij} \rangle = | \widetilde{\psi}_{ij} \rangle, \qquad (A4)$$

$$u_{A,i} \otimes u_{B,j} (M_{a|x}^{A_i} \otimes M_{b|y}^{B_j}) u_{A,i}^{\dagger} \otimes u_{B,j}^{\dagger} = \widetilde{M_{a|x}^{A_i}} \otimes \widetilde{M_{b|y}^{B_j}}$$

where  $|\widetilde{\psi}_{ij}\rangle$  and  $\{\widetilde{M_{a|x}^{A_i}}\}$ ,  $\{\widetilde{M_{b|y}^{B_j}}\}$  are the reference two-qubit strategy having support in the i-th (j-th) qubit block of Alice's (Bob's) Hilbert space.

Defining  $\Lambda_A := \bigoplus_l u_{A,l}^{\dagger}$  and  $\Lambda_B := \bigoplus_m u_{B,m}^{\dagger}$ , then the global state  $\rho = |\psi\rangle\langle\psi|$  is easily seen to be:

$$\begin{split} |\psi\rangle = \bigoplus_{i,j} \sqrt{\nu_{ij}} \, |\psi_{ij}\rangle &= \bigoplus_{ij} u_{A,i}^{\dagger} \otimes u_{B,j}^{\dagger} \sqrt{\nu_{ij}} \, |\widetilde{\psi}_{ij}\rangle \\ &= & \Lambda_{A} \otimes \Lambda_{B} \bigoplus_{i,j} \sqrt{\nu_{ij}} \, |\widetilde{\psi}_{ij}\rangle \, . \end{split} \tag{A5}$$

whereas the corresponding POVM elements are

$$\begin{split} M_{a|x}^{A} \otimes M_{b|y}^{B} &= \bigoplus_{i} M_{a|x}^{A_{i}} \otimes \bigoplus_{j} M_{b|y}^{B_{j}} \\ &= \left( \bigoplus_{i} u_{A,i}^{\dagger} \widetilde{M_{a|x}^{A_{i}}} u_{A,i} \right) \otimes \left( \bigoplus_{j} u_{B,j}^{\dagger} \widetilde{M_{b|y}^{B_{j}}} u_{B,j} \right) \\ &= \Lambda_{A} \otimes \Lambda_{B} \bigoplus_{i,j} (\widetilde{M_{a|x}^{A_{i}}} \otimes \widetilde{M_{b|y}^{B_{j}}}) \Lambda_{A}^{\dagger} \otimes \Lambda_{B}^{\dagger}. \end{split}$$

Without loss of generality, we may take the reference POVM elements for the first input (x = y = 0) as a measurement in the computational basis<sup>6</sup>

$$\widetilde{M_{a|0}^{A_i}} = |2i + a\rangle\langle 2i + a|, \quad \widetilde{M_{b|0}^{B_j}} = |2j + b\rangle\langle 2j + b| \quad \text{(A7)}$$

<sup>&</sup>lt;sup>5</sup> As with Footnote 3, to be mathematically precise, all the direct sums should be replaced by a regular sum in the following equations. Accordingly, each  $\Pi_i^A$  (and  $M_{a|x}^{A_i}$ ) is an operator acting on the full space, but only has support on the subspace of the i-th block. Likewise for  $\Pi_i^B$  and  $M_{b|n}^{B_j}$ 

<sup>&</sup>lt;sup>6</sup> If the intended reference measurements are not already in this form, one can make use of the promised 2-equivalence to choose, instead, a reference measurement that has this feature.

and the reference state  $|\widetilde{\psi}_{ij}\rangle$  in the same computational basis. What remains is to apply the local isometries

$$\Phi_A = \Phi' \circ \Lambda_A^{\dagger}, \quad \Phi_B = \Phi' \circ \Lambda_B^{\dagger}$$
(A8)

defined via

$$\Phi' |2s\rangle_K \mapsto |2s\rangle_{K'} |0\rangle_{K''}, 
\Phi' |2s+1\rangle_K \mapsto |2s\rangle_{K'} |1\rangle_{K''},$$
(A9)

for  $K \in \{A, B\}$ , likewise for K' and K''. It is then straightforward to see that these isometries indeed fulfill the self-testing requirement given in Eq. (12), thus completing the proof that the given extremal nonlocal correlation  $\vec{P}$  self-tests the reference state and measurement.

## Appendix B: All quantum correlations in Class 4b are local

As with the proof of Lemma III.1, we denote by  $\{|e_{a|x}\rangle\}$  ( $\{|f_{b|y}\rangle\}$ ) the orthonormal bases defining Alice's x-th (Bob's y-th) measurement. Then, the two ADZs in the upper-left block of Table IVb imply that the shared two-qubit pure state can be expressed as

$$|\Psi\rangle = \sum_{i=0}^{1} c_i |e_{i|0}\rangle |f_{i|0}\rangle, \quad \sum_{i=0}^{1} |c_i|^2 = 1.$$
 (B1)

Similarly, the ADZs in the lower-right block mean that the shared state can also be written as

$$|\Psi\rangle = \sum_{i=0}^{1} d_i |e_{i|1}\rangle |f_{i|1}\rangle, \quad \sum_{i=0}^{1} |d_i|^2 = 1.$$
 (B2)

Now let  $U_A$  and  $U_B$ , respectively, be the unitary connecting the bases of different local measurement settings, i.e.,

$$|e_{i|1}\rangle = \sum_{j} (U_A)_{ji} |e_{j|0}\rangle, |f_{i|1}\rangle = \sum_{j} (U_B)_{ji} |f_{j|0}\rangle,$$
 (B3)

where

$$U_A = \begin{bmatrix} \alpha & -\beta^* \\ \beta & \alpha^* \end{bmatrix}, \ U_B = \begin{bmatrix} \alpha' & -\beta'^* \\ \beta' & \alpha'^* \end{bmatrix}, \tag{B4}$$

and  $|\alpha|^2 + |\beta|^2 = |\alpha'|^2 + |\beta'|^2 = 1$ . Here and below, without loss of generality, we consider only unitary matrices of unit determinant.

Substituting the transformations of Eq. (B3) and Eq. (B4) into equation (B2), we obtain an expansion of  $|\Psi\rangle$  in the basis of  $\{|e_{i|0}\rangle|f_{j|0}\rangle\}$ . Specifically, the expansion coefficients for the term  $|e_{0|0}\rangle|f_{1|0}\rangle$  and  $|e_{1|0}\rangle|f_{0|0}\rangle$ , which ought to be zero according to Eq. (B1), are, respectively,

$$|e_{0|0}\rangle |f_{1|0}\rangle : d_0\alpha\beta' - d_1\beta^*\alpha'^* = 0,$$
  
 $|e_{1|0}\rangle |f_{0|0}\rangle : d_0\beta\alpha' - d_1\alpha^*\beta'^* = 0.$  (B5)

Hence, for  $d_0, d_1 \neq 0$ , their ratio is just a phase factor:

$$\frac{d_0}{d_1} = \sqrt{\frac{\alpha^* \alpha'^* \beta^* \beta'^*}{\alpha \alpha' \beta \beta'}} = e^{i\phi_d} :: \alpha \alpha' \beta \beta' \equiv |\alpha \alpha' \beta \beta'| e^{-i\phi_d}.$$
(B6)

Similarly, using the inverse unitaries  $U_A^\dagger$  and  $U_B^\dagger$ , we can write the basis vectors  $\{|e_{i|0}\rangle\,|f_{j|0}\rangle\}$  in the basis of  $\{|e_{i|1}\rangle\,|f_{j|1}\rangle\}$  in Eq. (B1) and arrive at the conclusion that  $c_0/c_1$  is also a phase factor, which we denote by  $e^{i\phi_c}$ .

This means that if  $|\Psi\rangle$  exhibits exactly the zeros distribution shown in Table IVb, it must be maximally entangled, i.e.,

$$\begin{split} |\Psi\rangle = & \frac{e^{i\phi_{0}}}{\sqrt{2}} [e^{i\phi_{c}} |e_{0|0}\rangle |f_{0|0}\rangle + |e_{1|0}\rangle |f_{1|0}\rangle] \\ = & \frac{e^{i\phi_{1}}}{\sqrt{2}} [e^{i\phi_{d}} |e_{0|1}\rangle |f_{0|1}\rangle + |e_{1|1}\rangle |f_{1|1}\rangle] \end{split} \tag{B7}$$

where  $e^{i\phi_0}$  and  $e^{i\phi_1}$  are global phase factors. Using Eq. (16), we then get

$$\langle A_0 B_0 \rangle = \langle \Psi | A_0 B_0 | \Psi \rangle = 1,$$

$$\langle A_0 B_1 \rangle = \langle \Psi | A_0 B_1 | \Psi \rangle = |\alpha|^2 - |\beta|^2,$$

$$\langle A_1 B_0 \rangle = \langle \Psi | A_1 B_0 | \Psi \rangle = |\alpha|^2 - |\beta|^2,$$

$$\langle A_1 B_1 \rangle = \langle \Psi | A_1 B_1 | \Psi \rangle = 1,$$
(B8)

which satisfy the CHSH inequality of Eq. (5) and all its relabeling. Hence, all  $\vec{P} \in \mathcal{Q}$  from Class 4a must be local.

## Appendix C: Robust self-testing of quantum strategies

In any real experiment, the observed measurement statistics are likely to differ from the exact self-testing quantum correlation. As such, for practical purposes, it is important to understand the robustness of any given self-testing statement against imperfections. To this end, we shall recall from [74, 75] the SWAP method and explain how it can be applied to determine the robustness of the self-testing results presented in Section III.

For the robust self-testing of a quantum state, we follow [74, 75] by considering local operators  $\Phi_{AA'}$  ( $\Phi_{BB'}$ ) that act jointly on the black-box system A(B) and the trusted auxiliary system A'(B'), i.e.,  $\Phi\rho_{AB} \otimes (|00\rangle \langle 00|)_{A'B'} \Phi^{\dagger}$ , where

$$\Phi = \Phi_{AA'} \otimes \Phi_{BB'}. \tag{C1}$$

As we see shortly, in the ideal case where Alice's (Bob's) actual observables  $A_i$  ( $B_i$ ) coincide with reference observables  $\widetilde{A}_i$  ( $\widetilde{B}_i$ ), the chosen local operator  $\Phi_{AA'}$  ( $\Phi_{BB'}$ ) becomes the operator that swaps the Hilbert spaces  $\mathcal{H}_A$  and  $\mathcal{H}_{A'}$  ( $\mathcal{H}_B$  and  $\mathcal{H}_{B'}$ ). Then the fidelity

$$F = \langle \widetilde{\psi} | \, \rho_{\text{SWAP}} \, | \widetilde{\psi} \rangle \,, \tag{C2}$$

between the reference state  $|\widetilde{\psi}\rangle$  and the "swapped" state

$$\rho_{\text{SWAP}} = \text{tr}_{AB} \left[ \Phi \rho_{AB} \otimes (|00\rangle\langle 00|)_{A'B'} \Phi^{\dagger} \right], \tag{C3}$$

naturally quantifies the closeness of relevant shared state in the black boxes  $\rho_{AB}$  to the reference state  $|\widetilde{\psi}\rangle$ .

To this end, let us first note from Section III that all reference observables considered are of the form:

$$\widetilde{A_i} = \cos(\theta_i)\sigma_x + \sin(\theta_i)\sigma_z.$$
 (C4)

Next, we define, for Alice's subsystem, the local operator:

$$\Phi_{AA'}(A_0, A_1) := U_{AA'}(A_0, A_1) V_{AA'}(A_0, A_1) U_{AA'}(A_0, A_1), \tag{C5a}$$

where the "controlled-NOT" gates are:

$$U_{AA'}(A_0, A_1) := \mathbb{1} \otimes |0\rangle\langle 0| + \widetilde{\sigma_{x,A}}(A_0, A_1) \otimes |1\rangle\langle 1|,$$

$$V_{AA'}(A_0, A_1) := \frac{\mathbb{1} + \widetilde{\sigma_{z,A}}(A_0, A_1)}{2} \otimes \mathbb{1}$$

$$+ \frac{\mathbb{1} - \widetilde{\sigma_{z,A}}(A_0, A_1)}{2} \otimes \sigma_x,$$
(C5b)

and following the form given in Eq. (C4), we define

$$\begin{split} \widetilde{\sigma_{x,A}}(A_0,A_1) &:= \frac{-\sin\theta_1\,A_0 + \sin\theta_0\,A_1}{\sin\theta_0\,\cos\theta_1\,-\cos\theta_0\,\sin\theta_1}, \\ \widetilde{\sigma_{z,A}}(A_0,A_1) &:= \frac{\cos\theta_1\,A_0 - \cos\theta_0\,\sin\theta_1}{\sin\theta_0\,\cos\theta_1\,-\cos\theta_0\,\sin\theta_1} \end{split} \tag{C5c}$$

Using Eq. (11), we can rewrite the local operator  $\Phi_{AA'}(A_0,A_1)$  in terms of the actual POVM elements, i.e.,  $\Phi_{AA'}(A_0,A_1) \to \Phi_{AA'}(\mathbb{1}_2,M_{0|0}^A,M_{0|1}^A)$ . Completely analogous definitions can be given for Bob's local operator  $\Phi_{BB'}$  in terms of his actual POVM elements  $M_{0|0}^B$  and  $M_{0|1}^B$ . Importantly, when the black boxes indeed implement the reference measurements,  $\widetilde{\sigma_{x,A}}(\widetilde{A_0},\widetilde{A_1}) = \widetilde{\sigma_{x,B}}(\widetilde{B_0},\widetilde{B_1}) = \sigma_x$  and  $\widetilde{\sigma_{z,A}}(\widetilde{A_0},\widetilde{A_1}) = \widetilde{\sigma_{z,B}}(\widetilde{B_0},\widetilde{B_1}) = \sigma_z$ , the local operators  $\Phi_{AA'}$ ,  $\Phi_{BB'}$  become the ideal operator that swap the blackbox subsystem and the respective auxiliary subsystem, and hence the fidelity of Eq. (C2) is unity.

More generally, by substituting Eq. (C1), Eq. (C3), Eq. (C5) and the analogous expressions for Bob's operator into Eq. (C2), we see that the fidelity of interest is a linear function of a subset of the moments  $\mu = \{ \operatorname{tr}(\rho_{AB}\mathbb{1}), \operatorname{tr}(\rho_{AB}M_{0|0}^A), \dots \}$ . To determine the robustness of the established self-testing statements (with respect to the reference state), we shall compute the worst-case fidelity by optimizing over all possible quantum realizations compatible with the observed value of  $\mathcal{S}_{\text{CHSH}}$  and some bounded deviation from the  $\mathcal{NS}$  boundary.

In practice, since we only have access to a converging hierarchy [15, 76, 77] of outer approximations to  $\mathcal{Q}$  (see also [51]), we solve, instead, the following semidefinite program (SDP) to obtain a lower bound on this worst-case fidelity:

$$\mathcal{F} = \min_{\mu \in \tilde{\mathcal{Q}}_{\ell}} \langle \widetilde{\psi} | \, \rho_{\text{SWAP}} \, | \widetilde{\psi} \rangle$$
 such that 
$$\sum_{a,b,x,y=0}^{1} (-1)^{xy+1+b+1} P(a,b|x,y) = \mathcal{S}_{\text{CHSH}}, \quad \text{(C6)}$$
 
$$P(a,b|x,y) \leq \varepsilon \, \forall \, P(a,b|x,y) \in \mathbb{P},$$

where  $\mathbb P$  is the set of conditional probabilities that are required to vanish in each Class,  $\varepsilon$  represents the maximum allowed deviation from this requirement, and  $\tilde{\mathcal Q}_\ell$  is, for example, the level- $\ell$  outer approximation of  $\mathcal Q$  described in [15] Not further that in this work, all reference states are some two-qubit state, which may be written in the Schdmit form:  $|\tilde{\psi}\rangle = c_0\,|00\rangle + c_1\,|11\rangle$  where  $c_0 \geq c_1$ . So, even if Alice and Bob share only the product state  $|00\rangle$  and hence do not violate any Bell inequality, they can already achieve a fidelity of  $c_0^2$ . In other words, for a nontrivial self-testing of the reference state  $|\tilde{\psi}\rangle$ , the fidelity has to be larger than  $c_0^2$ .

For the self-testing of measurements, we now consider the figure of merit:

$$T_A \equiv \frac{1}{2} \{ P_A(0|0, |e_{0|0}\rangle) + P_A(1|0, |e_{1|0}\rangle) + P_A(0|1, |e_{0|1}\rangle) + P_A(1|1, |e_{1|1}\rangle) \} - 1$$
(C7)

for Alice where

$$P_A(a|x,|\phi\rangle) = \operatorname{tr}\{M_{a|x}^A[\Phi_{AA'}(\rho_{AB} \otimes |\phi\rangle\langle\phi|)\Phi_{AA'}^{\dagger}]\}. (C8)$$

For Bob's measurements, we use a similar figure of merit  $T_B$  with  $P_A(a|x,|e_{a|x}\rangle)$  in Eq. (C7) replaced by  $P_B(b|y,|f_{b|y}\rangle)$  where the latter is defined in essentially the same way as  $P_A(a|x,|\phi\rangle)$  in Eq. (C8). Again, notices that when the black boxes indeed implement the reference measurements, each of these figure of merits becomes unity.

To determine the robustness of the established self-testing statements with respect to the reference measurements, we are interested in the the smallest possible value of these figures of merit given an observation of some correlation that deviates from the ideal self-testing correlation. For that matter, we again outer-approximate  $\mathcal Q$  by considering some superset  $\tilde{\mathcal Q}_\ell$  of  $\mathcal Q$  and solve the following SDPs to obtain a lower bound on the respective figures of merit:

$$\begin{split} \tau_i &= \min_{\mu \in \tilde{\mathcal{Q}}_\ell} T_i \\ \text{such that } \sum_{a,b,x,y=0}^1 (-1)^{xy+1+b+1} P(a,b|x,y) = \mathcal{S}_{\text{CHSH}}, \end{split} \tag{C9}$$
 
$$P(a,b|x,y) \leq \varepsilon \ \forall \ P(a,b|x,y) \in \mathbb{P}, \end{split}$$

for  $i \in \{A, B\}$ . Note also that if both parties' measurements are trivial, i.e.,  $M_{a|x}^A = M_{b|y}^A = \frac{\mathbb{1}_d}{2}$  for all a, b, x, y, and hence being jointly measurable, one can already achieve a score of  $T_A = T_B = 0$ . Thus, for a nontrivial self-testing of measurements, we must have  $\tau_A, \tau_B > 0$ .

# Appendix D: Quantum correlation giving maximal CHSH value in $Q_{3b}$ is a self-test

Here, we prove that  $\vec{P}_Q$  of Eq. (24b) gives the maximal CHSH violation in Class 3b. Moreover,  $\vec{P}_Q$  in not only an extreme point of Q, but also self-test the state and measurements of Eq. (23).

# 1. Maximal CHSH value for $\vec{P} \in \mathcal{Q}_{3b}$

With the measurement bases defined in Eq. (15) and Eq. (16), a general pure two-qubit state  $|\psi\rangle$  giving P(0,0|0,0)=P(1,1|0,0)=0 (cf. Table IVd) is:

$$|\psi\rangle = \cos\theta |e_{0|0}\rangle |f_{1|0}\rangle + e^{i\phi}\sin\theta |e_{1|0}\rangle |f_{0|0}\rangle.$$
 (D1)

Suppose the measurement bases are related via Eq. (B3) by

$$U_{A} = \begin{bmatrix} e^{i\gamma_{A}} \cos \alpha & e^{i\omega_{A}} \sin \alpha \\ -e^{-i\omega_{A}} \sin \alpha & e^{-i\gamma_{A}} \cos \alpha \end{bmatrix},$$

$$U_{B} = \begin{bmatrix} -e^{-i\omega_{B}} \sin \beta & e^{-i\gamma_{B}} \cos \beta \\ e^{i\gamma_{B}} \cos \beta & e^{i\omega_{B}} \sin \beta \end{bmatrix}.$$
(D2)

To arrive at nonlocal correlations, the local measurements should not commute, while the state must be entangled, thus:

$$\alpha, \beta, \theta \notin \left\{\frac{n}{2}\pi\right\}_{n \in \mathbb{Z}}.$$
 (D3)

Using Eq. (D1) and Eq. (D2) in Eq. (5) and Eq. (6), we arrive, respectively, at the CHSH Bell value:

$$S_{\text{CHSH}} = \zeta \prod_{j=\alpha,\beta,\theta} \sin 2j + 2\cos 2\alpha \cos^2 \beta + 2\sin^2 \beta \quad (D4)$$

and the joint conditional probability

$$P(1,0|1,1) = -\frac{\zeta}{4} \prod_{j=\alpha,\beta,\theta} \sin 2j + \sin^2 \alpha \cos^2 \beta \cos^2 \theta$$
$$+\cos^2 \alpha \sin^2 \beta \sin^2 \theta = 0$$
(D5)

where

$$\zeta := \cos\left(\gamma_A + \gamma_B + \omega_A + \omega_B + \phi\right) \tag{D6}$$

and the requirement that the latter probability vanishes follows from the structure of zeros shown in Table IVd.

Substituting the expression of  $\zeta$  obtained from Eq. (D5) into Eq. (D4) and simplifying give

$$S_{\text{CHSH}} = 2[\sin^2\theta(\cos 2\alpha - \cos 2\beta) + 1]. \tag{D7}$$

Note further that in the expression of P(1,0|1,1) in Eq. (D5), the variables  $\gamma_A,\gamma_B,\omega_A,\omega_B,\phi$  appear only in  $\zeta$ . If the constraint were to hold for some non-extremal value of the cosine function in  $\zeta$ , a slight variation of some of these parameters must lead to a negative value for the probability P(1,0|1,1). Hence, the constraint of Eq. (D5) must also imply an extremal value of  $\zeta$ , i.e.,  $\zeta=\pm 1$ . Using this in Eq. (D5) itself and simplifying lead to

$$\tan \alpha \pm \tan \beta \tan \theta = 0$$
 for  $\zeta = \mp 1$ . (D8)

Consider now the maximization of Eq. (D7) subjected to the constraint of Eq. (D8) via the Lagrangian functions  $\mathcal{L}_{\pm}$ :

$$\mathcal{L}_{\pm} = 2[\sin^2\theta(\cos 2\alpha - \cos 2\beta) + 1] + \lambda(\tan\alpha \pm \tan\beta \tan\theta),$$
(D9)

where  $\lambda$  is a Lagrange multiplier. Requiring that their vanishing partial derivatives vanish give

$$\frac{\partial \mathcal{L}_{\pm}}{\partial \alpha} = -4\sin^2\theta \sin 2\alpha + \lambda \sec^2\alpha = 0, \tag{D10}$$

$$\frac{\partial \mathcal{L}_{\pm}}{\partial \beta} = 4 \sin^2 \theta \sin(2\beta) \pm \lambda \sec^2 \beta \tan \theta = 0, \quad (D11)$$

and, upon the elimination of  $\lambda$ ,

$$\tan \theta = \mp \frac{\sin \beta \cos^3 \beta}{\sin \alpha \cos^3 \alpha}.$$
 (D12)

Together, Eq. (D12) and Eq. (D8) imply that extreme values of  $\mathcal{S}_{\text{CHSH}}$ , under the constraint of Eq. (D8), occur when  $\sin^2 2\alpha = \sin^2 2\beta$ , i.e.,  $\beta \in \left\{\frac{n\pi}{2} \pm \alpha\right\}_{n \in \mathbb{Z}}$ . Using this in Eq. (D7), one sees that  $\mathcal{S}_{\text{CHSH}}$  can be larger than 2 only if

$$\beta \in \left\{ (n + \frac{1}{2})\pi \pm \alpha \right\}_{n \in \mathbb{Z}}.$$
 (D13)

Substituting Eq. (D13) into Eq. (D8) and Eq. (D7), we see that the optimization problem reduces to

$$\max_{\theta,\alpha} \quad 4\cos 2\alpha \sin^2 \theta + 2$$
 s.t. 
$$\pm \tan^2 \alpha = \tan \theta,$$
 (D14)

where the sign in the constraint is positive if and only if the sign of  $\zeta$  is opposite to that of  $\alpha$  in Eq. (D13). By eliminating  $\alpha$  using the constraint or otherwise, we get

$$\pm \tan^3 \theta + \tan^2 \theta \pm \tan \theta - 1 = 0, \tag{D15}$$

whose solutions in the interval  $[-\pi, \pi]$  are<sup>7</sup>

$$\theta = \pm \theta_0, \quad \theta_0 := \tan^{-1} \frac{1}{3} \left( -1 - \frac{2}{\tau} + \tau \right) \approx 0.15851\pi$$
(D16)

where  $\tau$  is defined in Eq. (23c) and the sign associated with  $\tan \theta$  in Eq. (D15) [ $\theta_0$  in Eq. (D16)] follows that of the constraint in Eq. (D14). Accordingly, one finds from Eq. (D14) that admissible solutions of  $\alpha$  in the interval of  $[0, 2\pi)$  are

$$\alpha = \alpha_0, \ \alpha_0 + \pi$$
 and  $\alpha = \pi - \alpha_0, \ 2\pi - \alpha_0$  (D17a)

where

$$\alpha_0 := \tan^{-1} \sqrt{|\tan \theta_0|} \approx 0.20224\pi \tag{D17b}$$

Finally, using Eq. (D13), the extreme value of  $S_{\text{CHSH}}$  are due to the following choice of  $\beta$  in the interval  $[0, 2\pi)$ :

$$\beta = \frac{\pi}{2} \pm \alpha_0, \frac{3\pi}{2} \pm \alpha_0. \tag{D18}$$

It can be verified that all 32 legitimate combinations of  $\theta, \alpha, \beta$ , and  $\zeta$  [see, respectively, Eq. (D16), Eq. (D17), Eq. (D18), Eq. (D6) and the paragraph just below Eq. (D14)] give rise to the same correlation  $\vec{P}_{\rm Q}$  and hence the same maximal Bell value  $\mathcal{S}_{\rm CHSH} = 4 - 4(2\kappa_1 + \kappa_2) \approx 2.26977$ , where  $\vec{P}_{\rm Q}$ ,  $\kappa_1$  and  $\kappa_2$  are defined in Eq. (24b).

<sup>&</sup>lt;sup>7</sup> The other solutions of  $\theta \in [-\pi, \pi)$  are equivalent to the two presented in Eq. (D16) up to a global phase factor, see Eq. (D1).

# 2. Self-testing based on the maximally-CHSH-violating correlation in $Q_{3b}$

**Theorem D.1.** If the CHSH value given in Eq. (25) is observed alongside P(0,0|0,0) = P(1,1|0,0) = P(1,0|1,1) = 0, then the underlying state and measurements are equivalent to those given in Eq. (23) up to local isometries, i.e.,  $\vec{P}_Q$  self-tests this particular quantum realization.

*Proof.* In Appendix D 1, we have characterized all the qubit strategies leading to the maximal CHSH value attainable by  $\vec{P} \in \mathcal{Q}_{3b}$ . Next, we show that all these strategies are 2-equivalent to the one that performs on the reference state

$$|\tilde{\psi}\rangle = \cos\theta_0 |e_{0|0}\rangle |f_{1|0}\rangle + \sin\theta_0 |e_{1|0}\rangle |f_{0|0}\rangle$$
 (D19a)

the measurement [cf. Eq. (11)]

$$\begin{split} \widetilde{A}_0 &= \sigma_z, \quad \widetilde{A}_1 = \cos 2\alpha_0 \, \sigma_z - \sin 2\alpha_0 \, \sigma_x, \\ \widetilde{B}_0 &= \sigma_z, \quad \widetilde{B}_1 = -\cos 2\beta_0 \, \sigma_z - \sin 2\beta_0 \, \sigma_x, \end{split} \tag{D19b}$$

where  $\theta_0$ ,  $\alpha_0$  are defined, respectively, in Eq. (D16) and Eq. (D17),  $\beta_0 = \frac{\pi}{2} - \alpha_0$ , while  $|e_{0,1|0}\rangle$  and  $|f_{0,1|0}\rangle$  are taken as the  $\pm 1$  eigenstate of the Pauli matrix  $\sigma_z$  in Eq. (D19b).

To prove the lemma, we first note that the quantum strategy specified in Eq. (D19) is indeed an example of those characterized in Appendix D1 with  $\theta=\theta_0,\,\alpha=\alpha_0,\,\beta=\beta_0$ , and  $\phi=\gamma_A=\gamma_B=\omega_A=\omega_B=0$ . Next, note that for a general choice of these parameters, we have

$$A_0 = B_0 = \sigma_z = \begin{bmatrix} 1 & 0 \\ 0 & -1 \end{bmatrix},$$

$$A_1 = \begin{bmatrix} \cos 2\alpha & -e^{i(\gamma_A + \omega_A)} \sin 2\alpha \\ -e^{-i(\gamma_A + \omega_A)} \sin 2\alpha & -\cos 2\alpha \end{bmatrix}, \quad (D20)$$

$$B_1 = \begin{bmatrix} -\cos 2\beta & -e^{-i(\gamma_B + \omega_B)} \sin 2\beta \\ -e^{i(\gamma_B + \omega_B)} \sin 2\beta & \cos 2\beta \end{bmatrix}.$$

Moreover, for any fixed value of  $\gamma_A, \gamma_B, \omega_A, \omega_B$ , and  $\phi$ , all the 32 strategies characterized in Appendix D 1 related to different choices of  $\theta$ ,  $\alpha$ , and  $\beta$  only lead to different combination of signs in  $\tan \theta$ ,  $\sin 2\alpha$ ,  $\cos 2\alpha$ ,  $\sin 2\beta$ , and  $\cos 2\beta$ . The strategy of Eq. (D19), in particular, corresponds to a choice of positive sign for all these parameters.

With these observations in mind, it is not difficult to verify that the following unitaries

$$u_{A} = \begin{bmatrix} e^{-i\gamma_{A}} \frac{\cos \alpha}{|\cos \alpha|} & 0\\ 0 & e^{i\omega_{A}} \frac{\sin \alpha}{|\sin \alpha|} \end{bmatrix},$$

$$u_{B} = \begin{bmatrix} e^{i\gamma_{B}} \frac{\cos \beta}{|\cos \beta|} & 0\\ 0 & e^{-i\omega_{B}} \frac{\sin \beta}{|\sin \beta|} \end{bmatrix},$$
(D21)

transform the state of Eq. (D1) to the reference state of Eq. (D19a) via Eq. (13a), while ensuring that the observables of Eq. (D20) transform to those of Eq. (D19b) via Eq. (13b) for all a, x, b, y. To arrive Eq. (13a), we have also made use

of the relation of the sign of  $\zeta$  and  $\tan \theta$ , as mentioned above Eq. (D15). This completes the proof that all qubit strategies giving the maximal CHSH value in  $Q_{3b}$  are 2-equivalent.

The last ingredient that we need is the observation that  $\vec{P}_Q$  is extremal in Q, which follows from Fact II.2 and the fact in our characterization (see Appendix D 1) of *all* qubit strategies leading to the maximal CHSH violation in Class 3b, *only*  $\vec{P}_Q$  leads to this largest violation while complying with the constraint of Class 3b (cf. Table IVd). A direct application of Theorem II.4 using the extremality of  $\vec{P}_Q$  and the just-established 2-equivalence of all qubit strategies leading to this maximum completes the proof.

# Appendix E: Quantum correlation giving maximal CHSH value in $Q_{2b}$ is a self-test

# 1. Maximal CHSH value for $\vec{P} \in \mathcal{Q}_{2b}$

With the measurement bases defined in Eq. (15) and Eq. (16), we may write a general pure two-qubit state  $|\psi\rangle$  as

$$|\psi\rangle = \sum_{i=0}^{1} \left( c_{i0} |e_{i|0}\rangle |f_{0|0}\rangle + c_{i1} |e_{i|1}\rangle |f_{1|0}\rangle \right),$$
 (E1)

where  $\sum_{i,j=0}^{1}|c_{ij}|^2=1$ . Since  $\vec{P}\in\mathcal{Q}_{2b}$  satisfies P(0,0|0,0)=P(1,1|1,0)=0, these constraints imply, respectively, that  $c_{00}=c_{11}=0$ . We may thus restrict our attention to states of the form:

$$|\psi\rangle = \cos\theta |e_{1|0}\rangle |f_{0|0}\rangle + e^{i\phi}\sin\theta |e_{0|1}\rangle |f_{1|0}\rangle.$$
 (E2)

To proceed, let the local measurement bases be related via Eq. (B3) by

$$U_{A} = \begin{bmatrix} e^{-i\gamma_{A}} \cos \alpha & e^{-i\omega_{A}} \sin \alpha \\ -e^{i\omega_{A}} \sin \alpha & e^{i\gamma_{A}} \cos \alpha \end{bmatrix},$$

$$U_{B} = \begin{bmatrix} e^{-i\gamma_{B}} \cos \beta & e^{-i\omega_{B}} \sin \beta \\ -e^{i\omega_{B}} \sin \beta & e^{i\gamma_{B}} \cos \beta \end{bmatrix}.$$
(E3)

Using Eq. (E2) and Eq. (E3) in Eq. (5) and Eq. (6), we arrive at the Bell value:

$$S_{\text{CHSH}} = 2 - 4\sin^2\alpha(\cos^2\theta\sin^2\beta + \sin^2\theta\cos^2\beta) \quad \text{(E4)}$$
$$+ 2\zeta\sin2\theta\sin\alpha\sin2\beta$$

where  $\zeta := \cos(\omega_B + \gamma_B - \phi - \omega_A)$ .

Since the variables  $\phi$ ,  $\omega_A$ ,  $\omega_B$ ,  $\gamma_B$  appear in  $\mathcal{S}_{\text{CHSH}}$  only through  $\zeta$ , it is clear that for  $\mathcal{S}_{\text{CHSH}}$  to arrive at its largest value, we must have  $\zeta$  taking its extremal value of  $\pm 1$ , in accordance with the sign of  $\sin 2\theta \sin \alpha \sin 2\beta$ . We denote the resulting the Bell value, respectively, by

$$S_{\pm} = 2 - 4\sin^2\alpha(\cos^2\theta\sin^2\beta + \sin^2\theta\cos^2\beta)$$
 (E5)  
 
$$\pm 2\sin 2\theta\sin\alpha\sin 2\beta.$$

For a Bell violation to be possible (i.e., for either of  $\mathcal{S}_{\pm}$  to be larger than the local bound of 2), the local measurements should not commute and the state must be entangled. It can then be verified from Eq. (E2) and Eq. (E5) that the remaining variables must again satisfy Eq. (D3).

To find the largest value of  $\mathcal{S}_{\text{CHSH}}$ , we proceed using standard variational techniques by first computing the partial derivatives of  $\mathcal{S}_{\pm}$  with respect to  $\alpha$ ,  $\beta$ ,  $\theta$  and setting each of them to zero to get, correspondingly,

$$\sin \alpha = \pm \frac{\sin 2\theta \sin 2\beta}{4(\cos^2 \beta \sin^2 \theta + \sin^2 \beta \cos^2 \theta)},$$
 (E6)

$$\pm \sin 2\theta \cos 2\beta - \sin \alpha \sin 2\beta \cos 2\theta = 0,$$
 (E7)

$$\pm \cos 2\theta \sin 2\beta - \sin \alpha \sin 2\theta \cos 2\beta = 0.$$
 (E8)

By substituting Eq. (E6) into Eq. (E7) and Eq. (E8), and upon reduction, one eventually arrives at

$$|\sin \theta| = |\cos \theta| = |\sin \beta| = |\cos \beta| = \frac{1}{\sqrt{2}},$$
 (E9)

and hence

$$\sin \alpha = \pm \frac{1}{2} \sin 2\beta \sin 2\theta. \tag{E10}$$

By considering all possible values of  $\theta, \alpha, \beta \in [0, 2\pi)$  meeting these constraints, one finds that the maximal value of Eq. (E4) is  $\mathcal{S}_{\text{CHSH}} = \frac{5}{2}$ , which is attainable *iff*  $\alpha \in \{\frac{\pi}{6}, \frac{5\pi}{6}, \frac{7\pi}{6}, \frac{11\pi}{6}\}, \ \beta \in \{\frac{\pi}{4}, \frac{3\pi}{4}, \frac{5\pi}{4}, \frac{7\pi}{4}\}, \ \text{and} \ \theta \in \{\frac{\pi}{4}, \frac{3\pi}{4}, \frac{5\pi}{4}, \frac{7\pi}{4}\}.$  By explicit calculations, it can be verified that all these strategies give exactly  $\vec{P}_{\text{Q},3}$ . Since this is the only correlation in  $\mathcal{Q}_3$  giving this maximal value,  $\vec{P}_{\text{Q},3}$  is an extreme point of  $\mathcal{Q}$ .

# 2. Self-testing based on the maximally-CHSH-violating correlation in $Q_{2b}$

**Theorem E.1.** If the CHSH value of  $\frac{5}{2}$  is observed alongside the zeros shown in Table IVf, then the underlying state and measurements are equivalent to those given in Eq. (31) up to local isometries, i.e.,  $\vec{P}_{Q,3}$  self-tests this particular quantum realization.

*Proof.* From the unitaries given in Eq. (E3), the state of Eq. (E2) can be written explicitly in the bases of  $\{|e_{0|0}\rangle, |e_{1|0}\rangle\}$  and  $\{|f_{0|0}\rangle, |f_{1|0}\rangle\}$  as

$$|\psi\rangle = \cos\theta \,|e_{1|0}\rangle \,|f_{0|0}\rangle \tag{E11}$$

$$+e^{i\phi}\sin\theta(e^{-i\gamma_A}\cos\alpha|e_{0|0}\rangle-e^{i\omega_A}\sin\alpha|e_{1|0}\rangle)|f_{1|0}\rangle$$
,

whereas the corresponding observables read as:

$$A_0 = B_0 = \sigma_z = \begin{bmatrix} 1 & 0 \\ 0 & -1 \end{bmatrix},$$

$$A_1 = \begin{bmatrix} \cos 2\alpha & -e^{-i(\gamma_A + \omega_A)} \sin 2\alpha \\ -e^{i(\gamma_A + \omega_A)} \sin 2\alpha & -\cos 2\alpha \end{bmatrix}, \quad \text{(E12)}$$

$$B_1 = \begin{bmatrix} \cos 2\beta & -e^{-i(\gamma_B + \omega_B)} \sin 2\beta \\ -e^{i(\gamma_B + \omega_B)} \sin 2\beta & -\cos 2\beta \end{bmatrix}.$$

The quantum strategy of Eq. (31) is simply a special case of the above corresponding to  $\alpha = \frac{\pi}{6}$ ,  $\beta = \theta = \frac{\pi}{4}$ ,  $\gamma_A = \gamma_B = \omega_A = \omega_B = \phi = 0$ , giving

$$|\widetilde{\psi}\rangle = \frac{1}{\sqrt{2}} \left( \frac{\sqrt{3}}{2} |0\rangle |1\rangle + |1\rangle |0\rangle - \frac{1}{2} |1\rangle |1\rangle \right), \tag{E13a}$$

$$\widetilde{A}_0 = \sigma_z, \quad \widetilde{A}_1 = \frac{1}{2}\sigma_z - \frac{\sqrt{3}}{2}\sigma_x,$$

$$\widetilde{B}_0 = \sigma_z, \quad \widetilde{B}_1 = -\sigma_x.$$
(E13b)

Now, notice that for any fixed value of  $\gamma_A, \gamma_B, \omega_A, \omega_B$ , and  $\phi$ , all the 64 strategies characterized in Appendix E 1 related to different choices of  $\theta$ ,  $\alpha$ , and  $\beta$  only lead to different combination of signs in  $\tan\theta$ ,  $\sin2\alpha$ ,  $\cos2\alpha$ ,  $\sin2\beta$ , and  $\cos2\beta$ . The strategy of Eq. (E13), in particular, corresponds to a choice of positive sign for all these parameters.

It is then easy to verify that the following unitaries

$$u_{A} = \begin{bmatrix} e^{i\gamma_{A}} \frac{\cos \alpha}{|\cos \alpha|} & 0\\ 0 & e^{-i\omega_{A}} \frac{\sin \alpha}{|\sin \alpha|} \end{bmatrix},$$

$$u_{B} = \begin{bmatrix} e^{i\gamma_{B}} \frac{\cos \beta}{|\cos \beta|} & 0\\ 0 & e^{-i\omega_{B}} \frac{\sin \beta}{|\sin \beta|} \end{bmatrix},$$
(E14)

establish the 2-equivalence of all these qubit strategies. In other words, they transform, via Eq. (13), the state of Eq. (E11) and the observables of Eq. (E12), respectively, to the reference state of Eq. (E13a) and reference observables of Eq. (E13b) for all a, x, b, y. Note that in arriving at Eq. (E13a), we have also made use of the fact that the sign of  $\zeta = \cos(\omega_B + \gamma_B - \phi - \omega_A)$  follows that of of  $\sin 2\theta \sin \alpha \sin 2\beta$ .

Finally, a straightforward application of Theorem II.4 using the just-established 2-equivalence and the fact that  $\vec{P}_{Q,3}$  is extremal in  $\mathcal{Q}$  (see the end of Appendix E 1) completes the proof of the theorem.

# Appendix F: Quantum correlation giving maximal CHSH value in $Q_1$ is a self-test

To find the maximal CHSH violation for correlations in this Class, one may follow the procedure given in Appendix D 1 or Appendix E 1 by considering general qubit unitary matrices of unit determinant connecting the different measurement bases. For simplicity, however, we note that in the maximization of  $S_{\text{CHSH}}$ , it suffices to consider extreme points in Q, which can always be attained [78] in the CHSH Bell scenario by considering the observables:

$$A_0 = B_0 = \sigma_z,$$

$$A_1 = c_\alpha \sigma_z + s_\alpha \sigma_x, \quad B_1 = c_\beta \sigma_z + s_\beta \sigma_x,$$
(F1)

where  $c_{\alpha} := \cos \alpha$ ,  $c_{\beta} := \cos \beta$ ,  $s_{\alpha} := \sin \alpha$ ,  $s_{\beta} := \sin \beta$ , and  $\alpha, \beta$  are free parameters. Consider now the Bell operator [79] corresponding to the Bell inequality of Eq. (5)

$$\mathcal{B} = -A_0 \otimes B_0 - A_1 \otimes B_0 - A_0 \otimes B_1 + A_1 \otimes B_1. \quad (F2)$$

The maximal value of  $\mathcal{S}_{\text{CHSH}}$  is obtained by measuring the observables of Eq. (F1) on the eigenstate  $|\psi\rangle$  of  $\mathcal{B}$  giving the largest eigenvalue.

For correlations from Class 1, however, we also have the constraint  $P(0,0|0,0) = |\langle 00|\psi\rangle|^2 = 0$ . Thus, to find the maximal CHSH value achievable by  $\vec{P} \in \mathcal{Q}_1$ , we may consider  $|\psi\rangle$  to be an eigenstate of the principle  $3\times 3$  sub-matrix  $\mathcal{B}'$  of  $\mathcal{B}$  related to the span of  $\{|10\rangle, |01\rangle, |11\rangle\}$ , i.e.,

$$\mathcal{B}' = \begin{bmatrix} \tau & s_{\alpha}s_{\beta} & (1-c_{\beta})s_{\alpha} \\ s_{\alpha}s_{\beta} & \tau & (1-c_{\alpha})s_{\beta} \\ (1-c_{\beta})s_{\alpha} & (1-c_{\alpha})s_{\beta} & -\tau \end{bmatrix}.$$
 (F3)

where  $\tau := 1 + c_{\alpha} + c_{\beta} - c_{\alpha}c_{\beta}$ .

To compute the eigenvalue of  $\mathcal{B}'$ , note that its characteristic polynomial is

$$-\lambda^3 + \tau \lambda^2 + 4\lambda - 4c_{\alpha}^2 s_{\beta}^2 + 4c_{\alpha}(c_{\beta} - 1) - 4c_{\beta}(c_{\beta} + 1),$$
 (F4)

where  $\lambda$  is the eigenvalue. Using Mathematica, we find that the largest value of  $\mathcal{S}_{\text{CHSH}}$ , i.e., the largest real value of  $\lambda$  is  $\xi_3 \approx 2.6353$  with the unique parameters  $c_\alpha = c_\beta = \xi_1 \approx 0.2862$ , and the corresponding eigenvector is

$$|\psi\rangle = \sin\theta \left( \frac{\frac{\sin\alpha}{|\sin\alpha|} |0\rangle|1\rangle + \frac{\sin\beta}{|\sin\beta|} |1\rangle|0\rangle}{\sqrt{2}} \right) + \cos\theta |1\rangle|1\rangle,$$
(F5)

where  $\xi_1$ ,  $\xi_2$  and  $\xi_3$  are, respectively, the smallest positive roots of the cubic polynomials given in Eq. (37).

**Theorem F.1.** If the CHSH value of  $\xi_3$  is observed alongside P(0,0|0,0) = 0, then the underlying state and measurements are equivalent to those given in Eq. (36) up to local isometries, i.e.,  $\vec{P}_{0,4}$  self-tests this particular quantum realization.

*Proof.* Since the only remaining freedom is the sign of  $\sin \alpha$  and  $\sin \beta$ , it can be easily seen that the local unitary  $\sigma_z$  can be used to generate the required sign. Therefore, the correlation  $\vec{P}_{Q,4}$  which is the only one giving the maximal value of  $\mathcal{S}_{\text{CHSH}}$  in Class 1 is an extreme point and any quantum strategy realizing this correlation is 2-equivalent to the reference state and measurements given in Eq. (36). Since  $\vec{P}_{Q,4}$  is extremal in Q and all strategies realizing this maximum are 2-equivalent to the reference strategy, we may then apply Theorem II.4 to complete the proof.

# Appendix G: Non-exposed quantum extreme points on the no-signaling boundary

To arrive at the non-exposed property of the various example correlations given in Section III, we apply the method described in Appendix H of Ref. [35], i.e., we show that for each

of the self-testing  $\vec{P}$  described below, there is *no* Bell function  $\vec{B}$  such that it is the *unique* maximizer. For this matter, it suffices to show that for any Bell function where  $\vec{P}$  is a maximizer, a local extreme point gives also the same Bell value.

To this end, consider a vector  $\vec{M}$  with components

$$M(a,b|x,y) = M_{a|x}^A \otimes M_{b|y}^B.$$
 (G1)

Then a Bell operator [79] can be written as

$$\mathcal{B} = \vec{B} \cdot \vec{M},\tag{G2}$$

where  $\vec{B}$  is a vector of real numbers associated with an arbitrary Bell function.

Now, let  $\vec{B}$  be a Bell function maximized by the self-testing correlation  $\vec{P}$ . Since the corresponding reference state  $|\widetilde{\psi}\rangle$  is an eigenstate of the Bell operator  $\mathcal{B}$ , it follows from Eq. (G2) that any state vector  $|\phi\rangle$  orthogonal to  $|\widetilde{\psi}\rangle$ , i.e., satisfying  $\langle \phi | \widetilde{\psi} \rangle = 0$ , will result in a vector

$$\vec{T} \equiv \langle \phi | \vec{M} | \psi \rangle \tag{G3}$$

orthogonal to  $\vec{B}$ , giving  $\vec{B} \cdot \vec{T} = 0$ . Note also from Eq. (G1), Eq. (G3), and the completeness relations of POVM that  $\sum_{a,b} T(a,b|x,y) = 0$  for all x and y.

In our work, all  $|\widetilde{\psi}\rangle$  are two-qubit states, so one can always find three  $|\phi\rangle$  orthogonal to each reference state. For concreteness, we label all the sixteen local deterministic extreme points by  $j=0,1,\ldots,15$  such that

$$P_{d,j}(a,b|x,y) = \delta_{a,(j \bmod 2)x \oplus \lfloor \frac{j \bmod 4}{2} \rfloor} \delta_{b,\lfloor \frac{j \bmod 8}{4} \rfloor y \oplus \lfloor \frac{j}{8} \rfloor}. \tag{G4}$$

Then, if the optimum value of the following linear program

$$\begin{aligned} \max_{\vec{B} \in \mathbb{R}^8} & \vec{B} \cdot \vec{P} \\ \text{s.t.} & \vec{B} \cdot \vec{T}_i = 0 \quad \text{for} \quad i \in \{1, 2, 3\} \\ & \vec{B} \cdot \vec{P}_{d,j} \le 1 \quad \text{for} \quad j = 0, 1, \dots, 15, \end{aligned}$$
 (G5a)

is 1 and this bound is saturated by at least one of the  $\vec{P}_{d,j}$ , we obtain a proof that the self-testing correlation  $\vec{P}$  is non-exposed. To certify that the maximum value of Eq. (G5a) is upper bounded by 1, we make use of weak duality [80], namely the fact that any feasible solution of the linear program dual to Eq. (G5a), i.e.,

$$\min_{y_{j} \geq 0, z_{i} \in \mathbb{R}} \sum_{j=0}^{15} y_{j}$$
s.t. 
$$\sum_{j=0}^{15} y_{j} P_{d,j} + \sum_{i} z_{i} \vec{T}_{i} = \vec{P}$$
for  $i \in \{1, 2, 3\}$  and  $j = 0, 1, \dots, 15$ .

always provides an upper bound to the optimum value of Eq. (G5a). Note further that in Eq. (G5), each  $\vec{T}_i$  is obtained

Strictly, the current proof only applies to all quantum measurements of the form given in Eq. (F1). However, even more general measurements involving complex state and observables, such as those considered in the proof in Appendix D1 or Appendix E1 may be shown to be 2-equivalent to the reference strategy in a similar manner.

form a vector  $|\phi_i\rangle$  orthogonal to  $|\widetilde{\psi}\rangle$  via Eq. (G3). To complete the proof, it suffices to consider any subset  $\{|\phi_i\rangle\}$  such that the a dual feasible solution gives exactly 1.

In the following, we provide the  $\{|\phi_i\rangle\}$ ,  $\{\vec{T}_i\}$  and the corresponding dual variables  $\{y_j\}$ ,  $\{z_i\}$  needed for the proof of the non-exposed nature of  $\vec{P}_Q$ ,  $\vec{P}_{Q,2}$ ,  $\vec{P}_{Q,3}$  and  $\vec{P}_{Cabello}$ .

## 1. Class 3b

For the self-testing correlation  $\vec{P}_Q$  of Eq. (24b), which gives the maximal CHSH Bell violation in  $Q_{3b}$ , the corresponding reference state and measurements are provided in Eq. (23). To certify the non-exposed nature of  $\vec{P}_Q$ , it suffices to consider  $|\phi_1\rangle = |0\rangle|0\rangle$  as the state orthogonal to the reference state of Eq. (23a), which gives

$$\vec{T}_{1} = \begin{array}{c|cccc} & x = 0 & x = 1 \\ & 0 & 1 & 0 & 1 \\ \hline y = 0 & 0 & 0 & 0 & -t_{1} & t_{1} \\ \hline 1 & 0 & 0 & 0 & 0 & 0 \\ \hline y = 1 & 0 & -t_{2} & 0 & -t_{2} & 0 \\ 1 & t_{2} & 0 & t_{2} - t_{1} & t_{1} \\ \end{array},$$
(G6)

where

$$t_1 = \frac{1}{6} \left( \sqrt[3]{3\sqrt{33} - 17} - \frac{2}{\sqrt[3]{3\sqrt{33} - 17}} + 4 \right) \approx 0.2282$$

$$t_2 = \frac{1}{6} \left( \sqrt[3]{19 - 3\sqrt{33}} + \frac{4}{\sqrt[3]{19 - 3\sqrt{33}}} - 2 \right) \approx 0.4196$$
(G7)

The optimized  $\vec{B}$  has only the non-zero components  $B(a,b|1,0)=1 \quad \forall \ a,b.$ 

For the dual problem of Eq. (G5b), the assignment

$$y_{3} = \frac{1}{6} \left( \sqrt[3]{2 \left( 3\sqrt{33} + 13 \right)} - \frac{4 \cdot 2^{2/3}}{\sqrt[3]{3\sqrt{33} + 13}} - 1 \right) \approx 0.1478,$$

$$y_{8} = \frac{1}{3} \left( \frac{\sqrt[3]{11 \left( 3\sqrt{33} - 11 \right)}}{2^{2/3}} - \frac{22^{2/3}}{\sqrt[3]{3\sqrt{33} - 11}} + 2 \right) \approx 0.1041$$

$$y_{12} = \frac{1}{2} - y_{8}, \quad y_{6} = y_{3} - z_{1}t_{1},$$

$$y_{9} = 1 - y_{3} - y_{6} - y_{8} - y_{12}, \quad z_{1} = 2y_{3},$$
(G8)

and zero otherwise, is easily verified to be a feasible solution with a value of 1, thus showing that  $\vec{P}_{Q}$  is not exposed.

# 2. Class 2a

For the self-testing correlation  $\vec{P}_{Q,2}$  of Eq. (29), which gives the maximal CHSH violation in  $Q_{2a}$ , the corresponding reference state and measurements are, respectively,  $|\Phi_2^+\rangle$  and those provided in Eq. (28). To certify the non-exposed nature of

 $\vec{P}_{\rm Q,2}$ , we consider the singlet state  $|\phi_1\rangle=\frac{1}{\sqrt{2}}(|0\rangle|1\rangle-|1\rangle|0\rangle)$  as the state orthogonal to  $|\Phi_2^+\rangle$ , which gives

$$\frac{\frac{8}{\sqrt{3}}\vec{T}_{1}}{\vec{T}_{1}} = \frac{\begin{vmatrix} x = 0 & x = 1 \\ 0 & 1 & 0 & 1 \end{vmatrix}}{\begin{vmatrix} y = 0 & 0 & 0 & 0 & -1 & 1 \\ 1 & 0 & 0 & 1 & -1 & 1 \end{vmatrix}}$$

$$y = 1 \begin{vmatrix} 0 & -1 & 1 & -1 & 1 \\ 1 & 1 & -1 & 1 & -1 & 1 \end{vmatrix}$$
(G9)

The optimized  $\vec{B}$  has only the non-zero components  $B(1,b|0,0) = B(0,b|0,1) = 1 \quad \forall b$ .

For the dual problem of Eq. (G5b), the assignment

$$y_3 = y_6 = y_9 = y_{12} = \frac{1}{4}, \quad z_1 = \frac{1}{\sqrt{3}},$$
 (G10)

and zero otherwise, is easily verified to be a feasible solution with a value of 1, thus showing that  $\vec{P}_{Q,2}$  is not exposed.

# 3. Class 2b

For the self-testing correlation  $\vec{P}_{Q,3}$  of Eq. (32), which gives the maximal CHSH violation in  $Q_{2b}$ , the corresponding reference state and measurements are provided in Eq. (31). To certify the non-exposed nature of  $\vec{P}_{Q,3}$ , it suffices to consider the following states orthogonal to the reference state of Eq. (31),

$$|\phi_1\rangle = |0\rangle|0\rangle$$
,  $|\phi_2\rangle = \sin\alpha |0\rangle|1\rangle + \cos\alpha |1\rangle|1\rangle$ , (G11)

where  $\alpha = \frac{\pi}{6}$ . In this case,

$$8\sqrt{\frac{2}{3}}\vec{T}_{1} = \frac{\begin{vmatrix} x = 0 & x = 1 \\ 0 & 1 & 0 & 1 \end{vmatrix}}{y = 0 & 0 & 0 & 0 & -2 & 2 \\ 1 & 0 & 0 & 0 & 0 & 0 \end{vmatrix}},$$

$$y = 1 & 0 & -2 & 0 & -3 & 1 \\ 1 & 2 & 0 & 1 & 1 \end{vmatrix},$$

$$x = 0 & x = 1 \\ 0 & 1 & 0 & 1 \\ \hline 0 & 1 & 0 & 1 \\ \hline y = 0 & 0 & 0 & 0 & 0 & 0 \\ 2 & 2 & -2 & 0 & 0 \\ \hline y = 1 & 0 & 1 & -3 & 0 & -2 \\ 1 & 1 & 1 & 0 & 2 \end{vmatrix},$$
(G12)

and the optimized  $\vec{B}$  takes the form of

$$\vec{B} = \frac{ \begin{vmatrix} x = 0 & x = 1 \\ 0 & 1 & 0 & 1 \\ y = 0 & -b_1 & b_2 & 0 & 1 - b_1 - b_2 \\ 1 & 0 & b_2 & 0 & b_1 \\ y = 1 & 0 & b_2 & 0 & b_3 & b_1 \\ 1 & 2b_1 + b_2 & 0 & 0 & 0 \end{vmatrix},$$
 (G13)

where  $b_1 \approx 0.2197$ ,  $b_2 \approx 0.3410$ , and  $b_3 \approx 0.6590$ . For the dual program in Eq. (G5b), the assignment

$$y_2 = y_3 = y_{12} = y_{15} = \frac{1}{4}, \quad z_1 = z_2 = \frac{1}{\sqrt{6}},$$
 (G14)

and zero otherwise, is easily verified to be a feasible solution with a value of 1, thus showing that  $\vec{P}_{Q,3}$  is not exposed.

## 4. Class 2c

For the self-testing correlation  $\vec{P}_{\text{Cabello}}$  of Eq. (34), which gives the maximal CHSH violation in  $Q_{2c}$ , the corresponding reference state and measurements are provided in Eq. (35). To certify the non-exposed nature of  $\vec{P}_{\text{Cabello}}$ , it suffices to consider the following states orthogonal to the reference state of Eq. (35a)

$$\begin{aligned} |\phi_1\rangle &= k_2 |0\rangle |0\rangle - k_1 |0\rangle |1\rangle - k_3 |1\rangle |0\rangle + k_2 |1\rangle |1\rangle ,\\ |\phi_2\rangle &= k_3 |0\rangle |0\rangle - k_2 |0\rangle |1\rangle + k_2 |1\rangle |0\rangle - k_1 |1\rangle |1\rangle . \end{aligned}$$
(G15)

The exact analytic expression of  $\vec{T}_1$  and  $\vec{T}_2$  can be computed from Eq. (G3), Eq. (35), and Eq. (G15). Below, we provide their approximate form for ease of reference:

$$\vec{T}_{1} = \frac{\begin{vmatrix} x = 0 & x = 1 \\ 0 & 1 & 0 & 1 \end{vmatrix}}{y = 0 & 0 & 0 & -t_{1} & t_{2} & t_{3} \\ 1 & 0 & t_{1} & t_{4} & -t_{2} - t_{3} - t_{4} \end{vmatrix}},$$

$$y = 1 & 0 & t_{5} & t_{6} & t_{7} & 0 \\ 1 & -t_{5} & -t_{6} & t_{8} & -t_{7} - t_{8} \end{vmatrix}},$$

$$\vec{T}_{2} = \frac{\begin{vmatrix} x = 0 & x = 1 \\ 0 & 1 & 0 & 1 \\ 0 & 0 & -u_{1} & u_{2} & u_{3} \\ 1 & u_{1} & 0 & u_{4} - u_{2} - u_{3} - u_{4} \\ y = 1 & 0 & u_{5} - u_{6} & u_{7} & 0 \\ 1 & u_{6} & -u_{5} & u_{8} & -u_{7} - u_{8} \end{vmatrix}},$$
(G16)

where  $t_1 \approx 0.1507$ ,  $t_2 \approx 0.1319$ ,  $t_3 \approx -0.2826$ ,  $t_4 \approx 0.2891$ ,  $t_5 = 0.3202$ ,  $t_6 = 0.0909$ ,  $t_7 \approx 0.4112$ , and  $t_8 \approx 0.0098$  for  $\vec{T}_1$ , while  $u_1 \approx 0.4214$ ,  $u_2 \approx -0.2950$ ,  $u_3 \approx -0.1264$ ,  $u_4 \approx 0.2770$ ,  $u_5 \approx 0.0871$ ,  $u_6 \approx 0.3342$ ,  $u_7 \approx -0.2471$ ,  $u_8 \approx 0.2291$  for  $\vec{T}_2$ .

The optimized  $\vec{B}$  takes the form of

$$\vec{B} = \frac{\begin{vmatrix} x = 0 & x = 1 \\ 0 & 1 & 0 & 1 \end{vmatrix}}{\begin{vmatrix} y = 0 & 0 & b_1 & 0 & 0 & b_2 \\ 1 & 1 & 0 & 0 & 0 & 0 \end{vmatrix}},$$

$$y = 1 \begin{vmatrix} 0 & 0 & 1 & 0 & -b_2 \\ 1 & -b_3 & 0 & b_4 & b_5 \end{vmatrix},$$
(G17)

where  $b_1 \approx 0.6918$ ,  $b_2 \approx 0.4170$ ,  $b_3 \approx 0.2005$ ,  $b_4 \approx 0.1349$ , and  $b_5 \approx 0.0917$ .

For the dual program in Eq. (G5b), the assignment

$$y_{3} = \frac{1}{6} \left( -\sqrt[3]{53 - 6\sqrt{78}} - \frac{1}{\sqrt[3]{53 - 6\sqrt{78}}} + 7 \right) \approx 0.3427,$$

$$y_{12} = -\frac{\sqrt[3]{9 - \sqrt{78}}}{3^{2/3}} - \frac{1}{\sqrt[3]{3(9 - \sqrt{78})}} + 2 \approx 0.4786,$$

$$y_{15} = 1 - y_{3} - y_{12} \approx 0.1787,$$

$$z_{1} = -\sqrt{\frac{\zeta_{1} - \frac{133727}{\zeta_{1}} - 145}{48}} \approx -0.6414,$$

$$z_{2} = \frac{1}{6} \left( \zeta_{2} - \frac{23}{\zeta_{2}} - 11 \right) \approx 0.3855,$$

$$\zeta_{1} = \sqrt[3]{6827808\sqrt{78} + 35282447}, \ \zeta_{2} = \sqrt[3]{186\sqrt{78} + 1639},$$

and zero otherwise, is easily verified to be a feasible solution with a value of 1, thus showing that  $\vec{P}_{\text{Cabello}}$  is not exposed.

## 5. Class 1

For the self-testing correlation  $\vec{P}_{Q,4}$  of Eq. (38), which gives the maximal CHSH violation in  $Q_1$ , the corresponding reference state and measurements are provided in Eq. (36). To certify the non-exposed nature of  $\vec{P}_{Q,4}$ , it suffices to consider the following states orthogonal to the state of Eq. (36a)

$$|\phi_1\rangle = |0\rangle|0\rangle,$$

$$|\phi_2\rangle = \cos\theta \left(\frac{|0\rangle|1\rangle + |1\rangle|0\rangle}{\sqrt{2}}\right) - \sin\theta |1\rangle|1\rangle.$$
(G19)

The exact analytic expression of  $\vec{T}_1$  and  $\vec{T}_2$  can be computed from Eq. (G3), Eq. (35), and Eq. (G15). Below, we provide their approximate form for ease of reference:

$$\vec{T}_{1} = \frac{\begin{vmatrix} x = 0 & x = 1 \\ 0 & 1 & 0 & 1 \end{vmatrix}}{\begin{vmatrix} y = 0 & 0 & 0 & 0 & t_{1} & -t_{1} \\ 1 & 0 & 0 & 0 & 0 & 0 \end{vmatrix}},$$

$$y = 1 \begin{vmatrix} 0 & t_{1} & 0 & t_{2} & t_{3} \\ 1 & -t_{1} & 0 & t_{3} & -t_{2} - 2t_{3} \end{vmatrix}},$$

$$\vec{T}_{2} = \frac{\begin{vmatrix} x = 0 & x = 1 \\ 0 & 1 & 0 & 1 \\ 0 & 1 & 0 & 1 \end{vmatrix}}{\begin{vmatrix} y = 0 & 0 & 0 & u_{1} & u_{2} & u_{3} \\ 1 & u_{1} & -2u_{1} & u_{4} & -u_{2} - u_{3} - u_{4} \\ 1 & u_{3} & -u_{2} - u_{3} - u_{4} & u_{6} & -u_{5} - 2u_{6} \end{vmatrix}},$$

$$(G20)$$

where  $t_1 \approx 0.3298$ ,  $t_2 \approx 0.4766$ , and  $t_3 \approx -0.1468$ , for  $\vec{T}_1$ , while  $u_1 \approx 0.1111$ ,  $u_2 \approx 0.0397$ ,  $u_3 \approx 0.0715$ ,  $u_4 \approx -0.3113$ ,  $u_5 \approx -0.1429$ , and  $u_6 \approx -0.1288$  for  $\vec{T}_2$ .

The optimized  $\vec{B}$  takes the form of

$$\vec{B} = \begin{array}{c|cccc} & x = 0 & x = 1\\ & 0 & 1 & 0 & 1\\ \hline y = 0 & 0 & 1 & 1 + b_1 & -b_1 & 0\\ 1 & 1 & 1 & 0 & b_2\\ \hline y = 1 & 0 & 0 & 0 & 0 & b_4\\ 1 & 0 & b_3 & b_5 & 0 \end{array}, \tag{G21}$$

where  $b_1 \approx 0.4850$ ,  $b_2 \approx -0.1944$ ,  $b_3 \approx -0.6795$ ,  $b_4 \approx -0.7872$ , and  $b_5 \approx -0.3025$ .

For the dual program in Eq. (G5b), let  $\zeta_1 \approx 0.4450$ ,  $\zeta_2 \approx 0.7530$ , and  $\zeta_3 \approx 0.0677$  be the respective smallest positive roots of the following cubic polynomials:  $q_1(x) = x^3 - x^2 - 2x + 1$ ,  $q_2(x) = x^3 - 7x^2 + 14x - 7$ , and  $q_3(x) = x^3 - 32x^2 - 116x + 8$ . The assignment

$$y_3 = y_{12} = \zeta_1,$$
  $y_{15} = 1 - 2y_3 \approx 0.1099,$   $z_1 = -\sqrt{\zeta_2} \approx -0.8678,$   $z_2 = \sqrt{\zeta_3} \approx 0.2602,$  (G22)

and zero otherwise, is easily verified to be a feasible solution with a value of 1, thus showing that  $\vec{P}_{0.4}$  is not exposed.

# Appendix H: Proof of Corollary IV.3

From the proof of Corollary IV.2, we see that in maximizing the value of any Bell inequality in the CHSH Bell scenario by  $|\Phi_d^+\rangle$ , it suffices to consider correlations  $\vec{P} \in \mathcal{M}_d$  taking the form of Eq. (43). Let  $\vec{B}$  be the Bell coefficients associated

with the CHSH inequality of Eq. (5), then

$$\max_{\vec{P} \in \mathcal{M}_{d}} \vec{B} \cdot \vec{P}$$

$$= \max_{\vec{P}'_{i} \in \mathcal{M}_{2}, \vec{P}''_{j} \in \mathcal{L}, k \geq 0, \frac{d-k}{2} \in \mathbb{Z}^{+}} \frac{2}{d} \sum_{i=1}^{\frac{d-k}{2}} \vec{B} \cdot \vec{P}'_{i} + \frac{1}{d} \sum_{j=1}^{k} \vec{B} \cdot \vec{P}''_{j}$$

$$\leq \max_{k \geq 0, \frac{d-k}{2} \in \mathbb{Z}^{+}} \frac{2}{d} \sum_{i=1}^{\frac{d-k}{2}} \max_{\vec{P}'_{i} \in \mathcal{M}_{2}} \vec{B} \cdot \vec{P}'_{i} + \frac{1}{d} \sum_{j=1}^{k} \max_{\vec{P}''_{j} \in \mathcal{L}} \vec{B} \cdot \vec{P}''_{j}$$

$$= \max_{k \geq 0, \frac{d-k}{2} \in \mathbb{Z}^{+}} \frac{2}{d} \sum_{i=1}^{\frac{d-k}{2}} 2\sqrt{2} + \frac{1}{d} \sum_{j=1}^{k} 2$$

$$= \begin{cases} 2\sqrt{2} \left(\frac{d-1}{d}\right) + \frac{2}{d}, & d = \text{odd}, \\ 2\sqrt{2}, & d = \text{even.} \end{cases}$$
(H1)

These upper bounds are indeed attainable [see Eq. (5) of [81]], thus completing the proof that the maximal CHSH violation by  $|\Phi_d^+\rangle$  is given in the last line of Eq. (H1).

# Appendix I: Proof of Lemma IV.5

Let us begin by noting that the transposition operation preserves the hermiticity of a matrix. Then, from spectral theorem, we may write:

$$\begin{cases}
E_{0|0}^{\mathsf{T}} = \sum_{i=0}^{r^{0}} \lambda_{i} |e_{i}\rangle\langle e_{i}|, & 0 < \lambda_{i} \leq 1, \\
E_{1|0}^{\mathsf{T}} = \mathbb{1}_{d} - E_{0|0}^{\mathsf{T}}, & \\
F_{0|0} = \sum_{i=0}^{r^{1}} \lambda'_{i} |f_{i}\rangle\langle f_{i}|, & 0 < \lambda'_{i} \leq 1, \\
F_{1|0} = \mathbb{1}_{d} - F_{0|0}.
\end{cases} (I1)$$

where  $\lambda_i$  and  $\lambda'_i$  are, respectively, the nonvanshing eigenvalues of  $E_{0|0}^{\mathsf{T}}$  and  $F_{0|0}$ . Without loss of generality, suppose P(0,0|0,0)=0, then from Eq. (8), we get

$$\frac{1}{d} \text{tr}[E_{0|0}^{\mathsf{T}} F_{0|0}] = \frac{1}{d} \sum_{i=0}^{r^0} \sum_{j=0}^{r^1} \lambda_i \lambda_j' |\langle e_i | f_j \rangle|^2 = 0.$$
 (I2)

Notice that the RHS of Eq. (I2) is a sum of non-negative terms. The fact that this sum vanishes means that  $|\langle e_i|f_j\rangle|=0$  for all i,j, which means that  $E_{0|0}^{\scriptscriptstyle \rm T}F_{0|0}=0$ , i.e.,  $E_{0|0}^{\scriptscriptstyle \rm T}$  and  $F_{0|0}$  commute and hence can be diagonalized in the same basis.

<sup>[1]</sup> S. Popescu and D. Rohrlich, Found. Phys. 24, 379 (1994).

<sup>[2]</sup> G. Brassard, H. Buhrman, N. Linden, A. A. Méthot, A. Tapp, and F. Unger, Phys. Rev. Lett. 96, 250401 (2006).

<sup>[3]</sup> M. Navascués and H. Wunderlich, Proc. R. Soc. A 466, 881 (2009).

<sup>[4]</sup> M. Pawlowski, T. Paterek, D. Kaszlikowski, V. Scarani, A. Winter, and M. Zukowski, Nature 461, 1101 (2009).

<sup>[5]</sup> M. Navascués, Y. Guryanova, M. J. Hoban, and A. Acín, Nat. Commun. 6, 6288 (2015).

<sup>[6]</sup> J. S. Bell, Speakable and Unspeakable in Quantum Mechanics: Collected Papers on Quantum Philosophy, 2nd ed. (Cambridge University Press, 2004).

<sup>[7]</sup> J. S. Bell, Physics 1, 195 (1964).

<sup>[8]</sup> N. Brunner, D. Cavalcanti, S. Pironio, V. Scarani, and

- S. Wehner, Rev. Mod. Phys. 86, 419 (2014).
- [9] V. Scarani, Acta Physica Slovaca 62, 347 (2012).
- [10] A. Acín, N. Brunner, N. Gisin, S. Massar, S. Pironio, and V. Scarani, Phys. Rev. Lett. 98, 230501 (2007).
- [11] R. Colbeck, PhD thesis, arXiv:0911.3814 (2009).
- [12] S. Pironio, A. Acín, S. Massar, A. B. d. l. Giroday, D. N. Matsukevich, P. Maunz, S. Olmschenk, D. Hayes, L. Luo, T. A. Manning, and C. Monroe, Nature 464, 1021 (2010).
- [13] R. Gallego, N. Brunner, C. Hadley, and A. Acín, Phys. Rev. Lett. 105, 230501 (2010).
- [14] J.-D. Bancal, N. Gisin, Y.-C. Liang, and S. Pironio, Phys. Rev. Lett. 106, 250404 (2011).
- [15] T. Moroder, J.-D. Bancal, Y.-C. Liang, M. Hofmann, and O. Gühne, Phys. Rev. Lett. 111, 030501 (2013).
- [16] Y.-C. Liang, D. Rosset, J.-D. Bancal, G. Pütz, T. J. Barnea, and N. Gisin, Phys. Rev. Lett. 114, 190401 (2015).
- [17] S.-L. Chen, C. Budroni, Y.-C. Liang, and Y.-N. Chen, Phys. Rev. Lett. 116, 240401 (2016).
- [18] F. Baccari, D. Cavalcanti, P. Wittek, and A. Acín, Phys. Rev. X 7, 021042 (2017).
- [19] J.-D. Bancal, N. Sangouard, and P. Sekatski, Phys. Rev. Lett. 121, 250506 (2018).
- [20] M. Zwerger, W. Dür, J.-D. Bancal, and P. Sekatski, Phys. Rev. Lett. 122, 060502 (2019).
- [21] S.-L. Chen, C. Budroni, Y.-C. Liang, and Y.-N. Chen, Phys. Rev. A 98, 042127 (2018).
- [22] R. Arnon-Friedman and J.-D. Bancal, New J. Phys. 21, 033010 (2019).
- [23] S. Wagner, J.-D. Bancal, N. Sangouard, and P. Sekatski, Quantum 4, 243 (2020).
- [24] S.-L. Chen, H.-Y. Ku, W. Zhou, J. Tura, and Y.-N. Chen, Quantum 5, 552 (2021).
- [25] D. Mayers and A. Yao, Quantum Info. Comput. 4, 273 (2004).
- [26] I. Šupić and J. Bowles, Quantum 4, 337 (2020).
- [27] J. Wang, S. Paesani, Y. Ding, R. Santagati, P. Skrzypczyk, A. Salavrakos, J. Tura, R. Augusiak, L. Mančinska, D. Bacco, D. Bonneau, J. W. Silverstone, Q. Gong, A. Acín, K. Rottwitt, L. K. Oxenløwe, J. L. O'Brien, A. Laing, and M. G. Thompson, Science 360, 285 (2018).
- [28] W.-H. Zhang, G. Chen, X.-X. Peng, X.-J. Ye, P. Yin, X.-Y. Xu, J.-S. Xu, C.-F. Li, and G.-C. Guo, Phys. Rev. Lett. 122, 090402 (2019).
- [29] W.-H. Zhang, G. Chen, P. Yin, X.-X. Peng, X.-M. Hu, Z.-B. Hou, Z.-Y. Zhou, S. Yu, X.-J. Ye, Z.-Q. Zhou, X.-Y. Xu, J.-S. Tang, J.-S. Xu, Y.-J. Han, B.-H. Liu, C.-F. Li, and G.-C. Guo, Npj Quantum Inf. 5, 4 (2019).
- [30] S. Gómez, A. Mattar, I. Machuca, E. S. Gómez, D. Cavalcanti, O. J. Farías, A. Acín, and G. Lima, Phys. Rev. A 99, 032108 (2019).
- [31] J.-D. Bancal, K. Redeker, P. Sekatski, W. Rosenfeld, and N. Sangouard, Quantum 5, 401 (2021).
- [32] D. Wu, Q. Zhao, C. Wang, L. Huang, Y.-F. Jiang, B. Bai, Y. Zhou, X.-M. Gu, F.-M. Liu, Y.-Q. Mao, Q.-C. Sun, M.-C. Chen, J. Zhang, C.-Z. Peng, X.-B. Zhu, Q. Zhang, C.-Y. Lu, and J.-W. Pan, Phys. Rev. Lett. 128, 250401 (2022).
- [33] J. Barrett, N. Linden, S. Massar, S. Pironio, S. Popescu, and D. Roberts, Phys. Rev. A 71, 022101 (2005).
- [34] P. Horodecki and R. Ramanathan, Nat. Commun. 10, 1701 (2019).
- [35] K. T. Goh, J. Kaniewski, E. Wolfe, T. Vértesi, X. Wu, Y. Cai, Y.-C. Liang, and V. Scarani, Phys. Rev. A 97, 022104 (2018).
- [36] L. Hardy, Phys. Rev. Lett. 71, 1665 (1993).
- [37] R. Ramanathan, M. Horodecki, H. Anwer, S. Pironio, K. Horodecki, M. Grünfeld, S. Muhammad, M. Bourennane,

- and P. Horodecki, arXiv:1810.11648 (2018).
- [38] A. Rai, C. Duarte, S. Brito, and R. Chaves, Phys. Rev. A 99, 032106 (2019).
- [39] R. Rabelo, L. Y. Zhi, and V. Scarani, Phys. Rev. Lett. 109, 180401 (2012).
- [40] S. Kunkri, S. K. Choudhary, A. Ahanj, and P. Joag, Phys. Rev. A 73, 022346 (2006).
- [41] L.-M. Liang and C.-Z. Li, Phys. Lett. A 335, 371 (2005).
- [42] A. Rai, M. Pivoluska, M. Plesch, S. Sasmal, M. Banik, and S. Ghosh, Phys. Rev. A 103, 062219 (2021).
- [43] A. Rai, M. Pivoluska, S. Sasmal, M. Banik, S. Ghosh, and M. Plesch, Phys. Rev. A 105, 052227 (2022).
- [44] J. F. Clauser, M. A. Horne, A. Shimony, and R. A. Holt, Phys. Rev. Lett. 23, 880 (1969).
- [45] D. Collins and N. Gisin, J. Phys. A: Math. Gen. 37, 1775
- [46] A. Peres, Found. Phys. 20, 1441 (1990).
- [47] Y.-C. Liang, T. Vértesi, and N. Brunner, Phys. Rev. A 83, 022108 (2011).
- [48] T. Vidick and S. Wehner, Phys. Rev. A 83, 052310 (2011).
- [49] M. Junge and C. Palazuelos, Commun. Math. Phys. 306, 695 (2011).
- [50] B. G. Christensen, Y.-C. Liang, N. Brunner, N. Gisin, and P. G. Kwiat, Phys. Rev. X 5, 041052 (2015).
- [51] P.-S. Lin, T. Vértesi, and Y.-C. Liang, Quantum 6, 765 (2022).
- [52] C. Jebarathinam, J.-C. Hung, S.-L. Chen, and Y.-C. Liang, Phys. Rev. Research 1, 033073 (2019).
- [53] J. Kaniewski, Phys. Rev. Research 2, 033420 (2020).
- [54] N. Gigena and J. Kaniewski, Phys. Rev. A 106, 012401 (2022).
- [55] L. Masanes, Phys. Rev. Lett. 97, 050503 (2006).
- [56] T. Fritz, Found. Phys. 41, 1493 (2011).
- [57] K. F. Pál and T. Vértesi, Phys. Rev. A 80, 042114 (2009).
- [58] J. M. Donohue and E. Wolfe, Phys. Rev. A 92, 062120 (2015).
- [59] Y.-C. Liang, Correlations, Bell Inequality Violation & Quantum Entanglement, Ph.D. thesis, University of Queensland (2008).
- [60] R. F. Werner, Phys. Rev. A 40, 4277 (1989).
- [61] Y.-C. Liang, R. W. Spekkens, and H. M. Wiseman, Phys. Rep. 506, 1 (2011).
- [62] A. Fine, Phys. Rev. Lett. 48, 291 (1982).
- [63] Y. Xiang, Chin. Phys. B 20, 060301 (2011).
- [64] Y. Wang, X. Wu, and V. Scarani, New J. Phys. 18, 025021 (2016).
- [65] K.-S. Chen et al., "A generalization of Hardy's argument for nonlocality without inequality," (in preparation).
- [66] A. Cabello, Phys. Rev. A 65, 032108 (2002).
- [67] R. Cleve, P. Hoyer, B. Toner, and J. Watrous, in *Proceedings*. 19th IEEE Annual Conference on Computational Complexity, 2004. (2004) pp. 236–249.
- [68] Y.-C. Liang and A. C. Doherty, Phys. Rev. A 75, 042103 (2007).
- [69] G. M. D'Ariano, P. L. Presti, and P. Perinotti, J. Phys. A: Math. Gen. 38, 5979 (2005).
- [70] W. K. Wootters, Phys. Rev. Lett. 80, 2245 (1998).
- [71] J. Kaniewski, Phys. Rev. Lett. 117, 070402 (2016).
- [72] J. Kaniewski, (private communication).
- [73] J.-L. Chen, A. Cabello, Z.-P. Xu, H.-Y. Su, C. Wu, and L. C. Kwek, Phys. Rev. A 88, 062116 (2013).
- [74] T. H. Yang, T. Vértesi, J.-D. Bancal, V. Scarani, and M. Navascués, Phys. Rev. Lett. 113, 040401 (2014).
- [75] J.-D. Bancal, M. Navascués, V. Scarani, T. Vértesi, and T. H. Yang, Phys. Rev. A 91, 022115 (2015).
- [76] M. Navascués, S. Pironio, and A. Acín, New J. Phys. 10, 073013 (2008).
- [77] A. C. Doherty, Y.-C. Liang, B. Toner, and S. Wehner, in 23rd Annu. IEEE Conf. on Comput. Comp, 2008, CCC'08 (Los

Alamitos, CA, 2008) pp. 199-210.

- [78] T. Franz, F. Furrer, and R. F. Werner, Phys. Rev. Lett. **106**, 250502 (2011).
- [79] S. L. Braunstein, A. Mann, and M. Revzen, Phys. Rev. Lett.

**68**, 3259 (1992).

- [80] S. Boyd and L. Vandenberghe, *Convex Optimization*, 1st ed. (Cambridge University Press, Cambridge, 2004).
- [81] Y.-C. Liang and A. C. Doherty, Phys. Rev. A 73, 052116 (2006).